UNCLASSIFIED

AD NUMBER
AD135753
CLASSIFICATION CHANGES
TO: **UNCLASSIFIED**
FROM: **CONFIDENTIAL**
LIMITATION CHANGES
TO: **Approved for public release; distribution is unlimited. Document partially illegible.**
FROM: **Distribution authorized to U.S. Gov't. agencies and their contractors; Administrative/Operational Use; 20 MAY 1957. Other requests shall be referred to Office of Naval Research, 875 North Randolph Street, Arlington, VA 22203-1995. Document partially illegible.**
AUTHORITY
31 May 1969, DoDD 5200.10; ONR per DTIC form 55

THIS PAGE IS UNCLASSIFIED

THIS REPORT HAS BEEN DELIMITED
AND CLEARED FOR PUBLIC RELEASE
UNDER DOD DIRECTIVE 5200.20 AND
NO RESTRICTIONS ARE IMPOSED UPON
ITS USE AND DISCLOSURE.

DISTRIBUTION STATEMENT A

APPROVED FOR PUBLIC RELEASE;
DISTRIBUTION UNLIMITED.

Copy no. 3

CONFIDENTIAL

FC

THE AEROPHYSICS DEPARTMENT
OF
MISSISSIPPI STATE COLLEGE

CONFIDENTIAL

CONFIDENTIAL

APPLICATIONS OF HIGH EFFICIENCY BOUNDARY LAYER CONTROL

By

August Raspet

Research Report No. 10 20 May 1957

Conducted For

OFFICE OF NAVAL RESEARCH

Under

CONTRACT Nonr 978(01)

By

The Aerophysics Department

Mississippi State College

7/1/57 Cdr. C. J. Latimer

CONFIDENTIAL

APPLICATIONS OF HIGH EFFICIENCY BOUNDARY LAYER CONTROL

By

August Raspet
Aerophysics Department
Mississippi State College

Introduction

The purpose of this paper is to illustrate applications of the boundary layer control method which offer an ultimate in minimum power requirement and maximum aerodynamic effect, be that lift augmentation or drag reduction. The entire process can be analytically determined using Prandtl's form of the Karman boundary layer momentum equation:[1]

[illegible]

where [illegible] is the shear stress at the wall,
[illegible] is the velocity at the outer edge of the boundary layer,
[illegible] is the local suction velocity,
[illegible] is the velocity gradient in the flow direction,
[illegible] is the displacement thickness,
[illegible] is the momentum thickness,
[illegible] is the gradient of momentum thickness in the flow direction,
ρ is the fluid density, μ, its viscosity and $\nu = \frac{\mu}{\rho}$ is its kinematic viscosity.

The process of distributing suction by the momentum conservation process should not be confused with distributing suction by variable porosity with an effort to take care of the pressure variation over the surface. Such empirical techniques cannot meet the momentum demands of the boundary layer and, for this reason, either require excessive flows or do not delay the separation as far as rationally distributed suction by the momentum equation would.

By means of suction distributed according to the above relation, separation of the turbulent boundary layer is prevented up to the angle of attack for which the suction was computed. This being the case, the lift coefficient can be computed directly from the potential distribution which corresponds to that angle of attack.

It can therefore be seen that this method is entirely analytic, yielding the suction distribution along the chord, the power requirements for the suction, and the resultant lift coefficient. For maximum economy of suction power, however, the distributed suction method requires that the suction be initiated close to the leading edge of the wing. It also requires a porosity of the skin which is controlled in function of chordwise position.

At very high angles of attack, however, the flow around a curved surface - viz the leading edge - presents a problem which has been termed laminar separation. More aptly this should be called leading edge separation. A principle of containment of leading edge separation has been found effective in reducing the losses in the boundary layer due to this effect.[2]

Since the design method for distributed suction boundary layer control has already been published,[3] this paper will be devoted to the latest research in distributed suction boundary layer control and its applications.

Distributed Suction Boundary Layer Control on a Slotted Flap Wing

Distributed suction for high lift has been studied on an unflapped airfoil on a 1500 pound sailplane attaining a trimmed maximum lift coefficient of 2.3 for an air horsepower of 0.8. The technique has also been studied on a wing with a camber changing flap on a Piper Super Cub, Army L-21. Here, a power-off, boundary layer control-on, trimmed maximum lift coefficient of 3.0 was attained from 7.0 brake-horsepower which provided the suction and also cooled the engine.

In order to investigate the possibility of distributed suction in connection with a slotted flap an experimental arrangement was made on a Cessna, Army L-19. Suction was distributed along the forward portion of the airfoil. No suction was applied to the flap, since it was thought that the flow through the slot would provide sufficient energy for controlling the boundary layer on the flap.

When the airplane was flown, the power-on lift coefficient was found to be considerably increased from 2.8 to 4.9 with full power and full flap with 3 horsepower providing the suction. For the power-off condition, however, there was not sufficient elevator power to stall the plane. An exploration of the total head pressure at the elevator, Figure 1, showed that a separated, low energy wake from the wing immersed the horizontal tail.

Tuft studies of the wing and flap, Figure 2, revealed that the cause of the wake was the separated flow over the flap. However, by a slight modification of the flap gap, to make a convergent nozzle, the flow appeared to be attached to the airfoil, also shown in Figure 2. Yet the elevator still failed to develop sufficient moment to stall the wing.

When a tuft grid perpendicular to the flap was erected and the flow examined, Figure 3, the cause for the wake on the tail was revealed. In both cases, divergent and convergent slot gaps, the flow separated in a sandwich. The flow through the slot is shown to be a thin blanket capable of blowing the tufts, but entirely inadequate in momentum content to effect a full attachment of the outer flow.

The result of furt er examination of the complicated flows through the two slotted flap configurations is shown in Figures 4 and 5. The velocity profiles shown near the slot are revealing in that the velocities in the outer flow are much greater than those through the slot.

The conclusion to which this research leads is that since there is so much more energy on the outer flow than in that coming through the slot, distributed suction should be utilized to bring this high energy into the boundary layer. This implies simply a camber changing flap such as was used on the L-21.

Position on the Airfoil of Initiation of Boundary Layer Control Versus Efficiency

Since there appears to be some uncertainty regarding various lift augmentation systems, it may be instructive to look into the effect of initiating suction farther back on the airfoil. This may be necessary because of certain design compromises. Figure 6 shows the additional lift due to boundary layer control, in pounds per horsepower of suction energy, versus the position along the chord where distributed suction was started. In the momentum equation this means that more suction power is required because the momentum thickness has built up to a sizeable value ahead of the suction area. More power is required to bring into the boundary layer the energy needed to retain an attached flow. This illustration clearly shows the benefits of initiating suction early. It should be mentioned that in each of the cases the optimum suction distribution was analytically determined and the results experimentally measured. Moreover, it will be seen from this illustration that even for the suction far forward there is a fall off in trend. This may be due to the influence of the leading edge separation.

If we define an efficiency of lifting attained by various high lift methods as

$$\left(\frac{LIFT}{HP}\right)\left(\frac{W}{S}\right)^{\frac{1}{2}} = E = 19.1\left(\frac{\Delta C_L}{C_{L\,MAX}}\right)\left(C_L\right)^{\frac{1}{2}}$$

we can display the results of various systems of lift augmentation, Figure 7. By this definition the effect of wing loading can be eliminated. There can be no doubt about the high efficiency of distributed suction boundary layer control.

There are still those who feel, however, that although suction requires less power, it yields smaller lift coefficients than blowing. Flight measurements of blowing have yet to reach even the simple unflapped suction airfoil maximum lift coefficient of 2.3. Perhaps, for some reason, tunnel measurements of blowing on small scale models yielded an over optimistic result.

A comparison of various flight-measured lift augmentation systems is shown in Figure 8. In this logarithmic plot one can easily see the trend in power requirements for the various systems. In some cases data previously published can be used to predict the performance of an experimental system when installed on a heavier airplane (e. g. YC-134 versus the Göttingen AF-2 all suction system.)

Landing Problems of High Lift Airplanes

Although lift coefficients on boundary layer control airplanes have still not reached the optimistic values extrapolated from two-dimensional tunnel data, they have reached values such that special techniques for landing must be studied. Figure 9 shows various techniques which tend to shorten the total landing distance over a 50 foot obstacle. An effective boundary layer control system should offer another parameter which can be used to advantage in shortening the landing distance.

Figures 10 and 11 show that the total landing distance over a 50 foot obstacle decreases with increasing lift coefficient. This is to be expected from a consideration of the total energy which must be dissipated during the landing. Figure 12 shows, however, that such is not the case for the L-19 with and without boundary layer control (Cessna 319A using Arado System).[4, 4a] This data clearly shows that influences other than that of lift coefficient enter into the short field landing with this airplane. In particular, this airplane suffered from a sharp leading edge stall. As a result, the pilot could not safely fly it close to maximum lift coefficient at which the induced drag would have been high enough to steepen the approach.

How much of the available lift coefficient a pilot dares to use on landing is a matter of both pilot skill and instrumentation. In order to provide the pilot with information which progressively warns him of the reserve lift, we have developed a reserve lift indicator, Figure 13. By continuously measuring the thickness of the boundary layer, this instrument is able to warn the pilot when he is approaching the stall. As the layer thickens the warning noise becomes louder and louder reaching an uncomfortable level just at the stall. Approaches can be made at 80 per cent of $C_{L\ max}$. For a skilled short field pilot, an adjustment may be made to give the first warning at 90 per cent of $C_{L\ max}$.

In Figure 14 is shown the calibration for this instrument when installed on an Army L-17B Navion. With this instrument, short field approaches can safely be made at an approach speed of 57 miles per hour instead of the usual 75 miles per hour.

This instrument should prove very useful when making approaches on the back side of the power polar which will be necessary with boundary layer control airplanes.

High Lift Applications

It may be of interest to manufacturers of assault airplanes to look at Figure 8 in order to determine the suction power required to increase the power-off maximum lift coefficient from a value of 2.0 to 4.0 for an airplane of the size of the C-123 at a gross weight of 55,000 pounds. Using the distributed suction system we obtain an efficiency of 1,000. With a wing loading of 40 pounds per square foot, the lift per horsepower is 150. Since the additional lift required to double the lift coefficient is 27,500 pounds, we find that a suction power of 183 horsepower is needed. For the Arado System the suction power required would be at least twice as much as the distributed suction value, provided leading edge separation does not become a limiting factor as happens on the Cessna 319A. As a matter of fact, the Air Force C-123, equipped with the Arado System, used two Aspin turbofan engines with a total of 900 horsepower.

It should be noticed in Figure 15 that, for the suggested C-123 boundary layer control system, the suction fan in each wing is supplied power (through a hydraulic driving pump) by the engine in the opposite wing. In the event of a single engine failure the minimum single engine control speed will therefore be much lower than with an uncrossed system.

For many multi-engine airplanes, especially the higher powered military planes, the asymmetrical power failure becomes a serious problem in short field landing and take-off. An obvious solution is inter-connection of power plants. Another which tends to alleviate the situation consists of oppositely rotating propellers. On the Beech, Army L-23, the single engine minimum control speed is 85 miles per hour with left engine out and 73 miles per hour with the right engine out. However, the stall speed - flaps down, power-on - is 54 miles per hour.

Since high lift will reduce the stall speed without improving the single engine minimum control speed, it is necessary to give some consideration to such schemes as the cross-over system mentioned for the C-123 as well as to means for improving directional control at low speeds. In Figure 16 is shown an approach wherein distributed suction is applied to the vertical tail surfaces. For the case of no yaw, the vertical tail with rudder deflected 25 degrees yields a maximum lateral force coefficient (corresponding to C_L for a wing) of 0.66. Yet with distributed suction the lateral force coefficient can be raised to 2.18 with an expenditure of suction power of only 1.1 horsepower on each side of the vertical tail surface.

It should be mentioned that this example of distributed suction boundary layer control is a clear-cut demonstration of the beauty of the distributed suction momentum conservation method. First, the pressure distribution around the deflected rudder-fin combination is computed by Moriya's method.[5] Next, from the velocity gradients and the momentum equation, the suction inflow velocity is computed. Then from this velocity and selected hole sizes, the distribution of perforations is determined. The internal pressure is selected so that excessive pressure drops through the surface are not encountered. When such a suction surface is built, separation being prevented, the original pressure distribution will be retained and the resultant force coefficient realized.

Ducted Propeller

An earlier work[3] has already manifested the need for high static thrust and high propulsive efficiencies at low speeds for high lift airplanes. Classical solutions to this problem consist either of large diameter, slow rotating propellers, as effected on the Helio-plane and Fieseler Storch, or of high power turboprop engines as are presently being used on STOL and VTOL airplanes. Where fuel economy is an important consideration, however, power extravagance is not permissible. The weight of large diameter propellers, together with the heavy landing gear necessitated thereby, and the torque which such propellers produce are sufficient reasons for studying the more attractive small diameter ducted propeller. Propeller tip noise reduction also results from the use of the ducted propeller.[6]

Since the duct presents quite a lateral area, it is not well suited to tractor propellers. For this reason, and because slip stream turbulence is eliminated over the nose, the pusher ducted propeller has been the subject of study at the writer's institute. Figure 17 shows a duct of 5.5 feet internal diameter mounted on an AG-14 pusher of 90 horsepower.

The results of static thrust measurements and distribution of total head rise behind the propeller for the non-ducted propeller and the ducted propeller are shown in Figure 18. In spite of the large increase of static thrust, the ducted propeller on this airplane, nevertheless, has not reached expected performance. Further work on the design of the propeller-duct combination is needed in order to realize the full potential of the ducted propeller.

In Figure 19 are shown the results of the available ducted propeller static thrust measurements so far made. Two outstanding and well-known tests are those of Kruger[7] and Platt.[8] These and the theoretical curves should provide us with a goal in our efforts toward efficient application and full understanding of the ducted propeller. It will be seen that the ducted propeller on the AG-14 is really performing no better than many open propeller tractors. This being the case we have need for additional research to determine the causes for not attaining better static thrust. One cause has already been found - the separation of the flow around the leading edge of the duct. By means of distributed suction on this duct the static thrust was increased by 60 pounds. This was done with an energy expenditure of 5 horsepower. When the flow around the leading edge is attached, however the inflow velocity into the outer edges of the propeller is so high that the angle of attack on these portions of the blade is diminished to a value such that little work is being done in accelerating the flow over the duct. This experiment clearly shows that the blade tip must be twisted to high blade angles so that high velocities are obtained around the duct's leading edge. It is these velocities which result in duct thrust and also in leading edge separation which must be alleviated by suction.

Examining Figure 19 again we see that Propeller Number 3 in a small 12 inch duct powered by a 2.5 horsepower motor is approaching the theoretical shrouded propeller curve. This small ducted propeller has no boundary layer control, merely a generous leading edge radius and five blades aimed at accelerating the flow around the duct's leading edge. The test arrangement for this small ducted propeller is shown in Figure 20.

Refinements in the design of a ducted propeller can be effected by plotting the shroud thrust coefficient versus the total thrust, Figure 21. The shroud thrust is easily obtained from an integration of the pressure distribution around the shroud and the propeller thrust from the total head rise through the propeller. For the 12 inch ducted propeller, the following data was obtained:

Shroud thrust	2.4 lbs.
Propeller thrust	2.3 lbs.
Total	4.7 lbs.
Measured total	5.0 lbs.

$$\frac{\text{Shroud thrust}}{\text{Total thrust}} = 48\%$$

These data show that the sum of the shroud thrust and propeller thrust accounts for all but 6 per cent of the thrust. Efforts will be made to account for this deficit.

Figure 21 shows that at peak thrust the shroud provides about 65 per cent of the thrust of the combination. When the propeller stalls, this ratio rises but the total thrust falls.

Our work on ducted propellers points the way for additional research efforts. Presently, an aluminum propeller is being carved which will be twisted in such a way as to load the propeller tips efficiently. A higher suction pressure will insure separation-free flow around the duct's leading edge. Additional research, to determine the influence of the wake of the fuselage, is now under way, using boundary layer control on the blunt after-body.

Diffuser Boundary Layer Control

In aerodynamics there are many cases requiring a transformation of velocity energy to pressure energy. Unfortunately, because of viscous effects, this transformation means that diffusion is not as effectively accomplished as in electricity where a transformer does the job. Where space is limited, a short wide angle diffuser is used. In general, any angle beyond 7 degrees, included, results in a poor pressure recovery efficiency. Since distributed suction boundary layer control over an airfoil offers a means of accomplishing the same result, an experimental diffuser of 30 degrees and 4:1 area ratio was built with a double wall on the conical surface in order to exhaust the air off the inner wall.

By means of suction amounting to 3 per cent of the main flow, the energy efficiency was raised from 50 to 96 per cent. The turbulence in the flow was also reduced since no free vortices formed on the wall. Figure 22 shows the turbulence by means of a time exposure of a series of balsa vanes free to oscillate on a wire. The breadth of the oscillation pattern is an indication of the turbulence. The photo with boundary layer control on shows how smooth the flow is when compared to flow with boundary layer control off. A comparison of the velocity profiles at the diffuser exit is shown in Figure 23.[9]

An understanding of the diffuser process will lead to better internal ducting on boundary layer control systems, to higher circulation around ducts of ducted propellers, to improved efficiency of axial compressor combustion chambers, and to solutions to other problems of this nature. This same diffuser problem, though inverted, exists on blunt fuselage after-bodies and on blimps.

Propeller Boundary Layer Control

The certainty with which distributed suction boundary layer control has permitted us to attack various flow problems finally enticed us into studying boundary layer control on open propellers. A clue to this problem appeared to be a possible reduction in the effect of the tip vortex on the static thrust. It was found, however, that the very strong radial flows toward the tip resulted in a three-dimensional boundary layer. Suction of small quantities had little or no effect on this three-dimensional boundary layer. The power added for suction gave a thrust increase which was just about equalled by the same power added to the propeller shaft. In other words, no power profit was obtained.

Figure 24 shows microflash tuft photos of a revolving hollow propeller blade with different areas of perforated suction. It is evident from Figure 24B that the radial flow is somewhat reduced by suction. There is, as pointed out above, no over-all power profit, but instead, a possible weight increase, and certainly, an increase in complication.

This propeller boundary layer control research teaches us that we will do not understand how to control the three-dimensional boundary layer. This type of flow occurs on propeller blades, swept wings and bodies of revolution. It merits some fundamental work.

Directional Stability on Tailless Aircraft

On tailless aircraft, directional stability has been marginal because the moment arm of the vertical tail has been of necessity kept small. Canted tip fins have been used, but these introduce so much drag that the advantages of the tailless configuration are lost. Obviously a tailless aircraft having a configuration similar to a bird - i. e. no vertical tail surfaces - is most desirable from the aspect of keeping drag to a minimum.

It would be possible to use a yaw detector connected to a servo valve controlling the boundary layer control suction air in the wings in an asymmetrical manner. The behavior of such a scheme has been demonstrated on our high lift boundary layer control sailplane by turning off the suction pumps on one wing and keeping them in operation on the other. Strong rolling and favorable yawing result.

For dependability, however, it is desirable to have an inherent stability dependent only on the geometry of the aircraft. For this reason, an investigation was made of the nature of the boundary layer on the Hoerner tips of a Plank Sailplane. Tuft observations showed that yawing involved a separation of the tufts which tended to increase the drag on the retreating wing. Such a craft would be directionally unstable.

By designing the Hoerner tip with positive rake it was possible to reverse the tendency to separate, thereby attaining positive directional stability, Figure 25. In fact, the stability increased with lift coefficient, which is a desirable feature for landing and take off.

This example while not one of suction boundary layer control is a good illustration of the facility of boundary layer technology in handling stability problems resulting from boundary layer misbehavior.

Conclusions

In the fast developing field of boundary layer control there has been a lot of wishful thinking - a seeking, if you please, of some bit of magic by which to take us beyond the present art in aerodynamics. That bit of magic, it cannot be gainsaid, has nevertheless been ours for a generation; for it was about 1925 that Prandtl[10] placed the suction term into von Karman's well-known boundary layer momentum equation.[11]

There are still those, however, who would use a less fundamental way than that offered by Prandtl. They seek a way of overcoming what are felt to be faults in the distributed suction system. If we are to have the high efficiency of the distributed suction process, we must also make the holes. The drilling process can be automatized by clever tool engineers. True, these holes will ice over in a freezing rain but replacing the suction flow with heated outflow offers the possibility of an excellent de-icing system. If design problems must be solved in order to provide space for ducting, their solutions surely are within the scope of our engineering abilities.

The author hopes the various applications of high efficiency distributed boundary layer control will inspire engineers to begin using this tool, the new parameter in aerodynamics.

References

1. Raspet, August, "Momentum Conservation In Boundary Layer Control," Paper Presented at the Boundary Layer Control Symposium, Naval Ordnance Laboratory, White Oaks, Maryland, June 24, 1953.

2. Cornish, Joseph J., III, "Prevention of Turbulent Separation by Suction Through a Perforated Surface," Research Report No. 7, October 13, 1953.

3. Raspet, A.; Cornish, J. J., III and Bryant, G. D., "Delay of the Stall by Suction Through Distributed Perforations," Institute of Aeronautical Sciences, January 23-26, 1956.

4. Fisher, Gertsen, Wise, Walter, Little, McGuckin, "Flight Test Results on the Use of High Lift Boundary Layer Control Applied to a Modified Liaison Airplane," Cessna Aircraft Co., Report No. 1339-7, March 31, 1956.

4a. Edwards AFB Flight Test Data on L-19.

5. Moriya, T., "A Simple Method of Calculating the Aerodynamic Characteristics of an Arbitrary Wing Section," Journal of the Society of Aeronautical Science, Japan, Vol. 5, 1938.

6. Hubbard, H., "Sound Measurements for Five Shrouded Propellers at Static Conditions," NACA TN 2024, 1950.

7. Kruger, W., "On Wind Tunnel Tests and Computations Concerning the Problem of Shrouded Propellers," NACA TN No. 1202, February, 1949.

8. Platt, Robert J., Jr., "Static Tests of a Shrouded and an Unshrouded Propeller," NACA RM No. L7H25, February 9, 1948.

9. Moon, I Man, "Boundary Layer Control by Distributed Suction on a Wide Angle Conical Diffuser," Paper Presented at the Southeastern Regional Student Conference of the Institute of Aeronautical Sciences, April 18-19, 1957.

10. Prandtl, L., "The Mechanics of Viscous Fluids," in Durand (Ed.), Aerodynamic Theory, Vol. III, Divisions F-I, pp. 117-119, 1943.

11. von Karman, Th., "Über laminare und turbulente Reibung," ZAMM, 1, 233 (1921), NACA Tech. Memo. No. 1092.

Illustrations

WAKE OF L-19 WING AT $C_L = 1.87$

$q = 1.23'' \ H_2O$

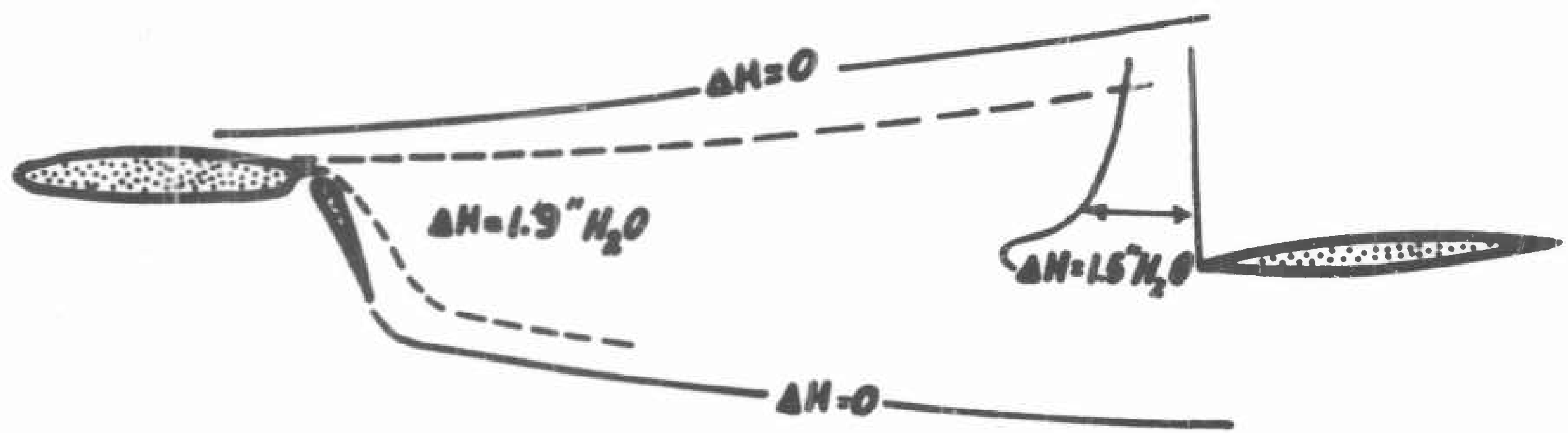

- FULL FLAP
- IDLE POWER
- B.L.C. ON

CONFIDENTIAL

FIG. 1

CONFIDENTIAL

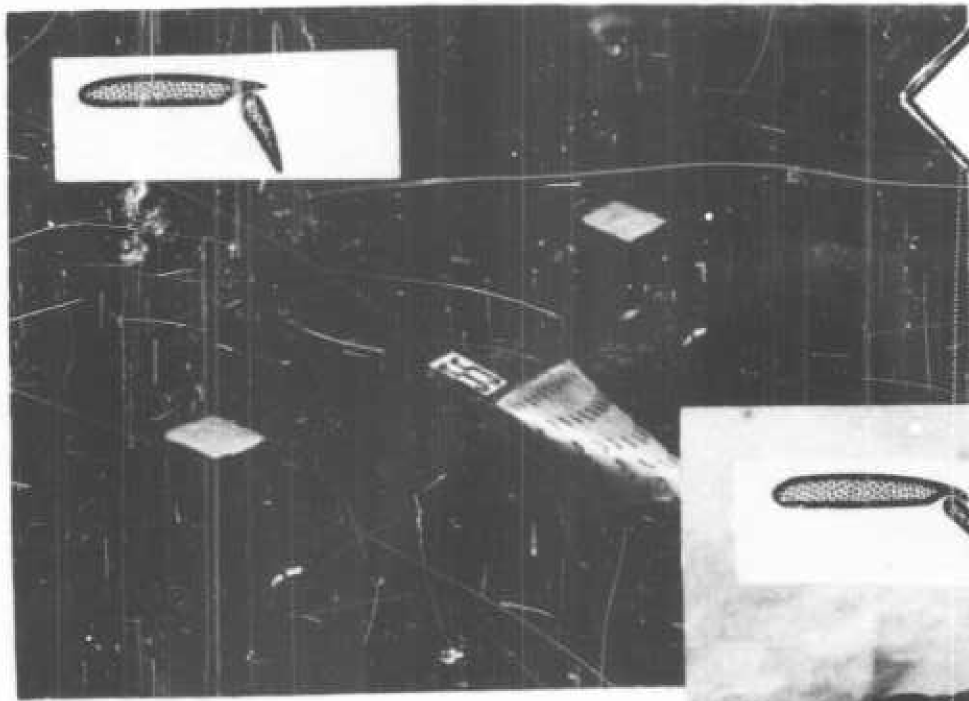

FLOW OVER AIRFOIL. BOUNDARY LAYER CONTROL ON FULL FLAP IDLE POWER GLIDE.

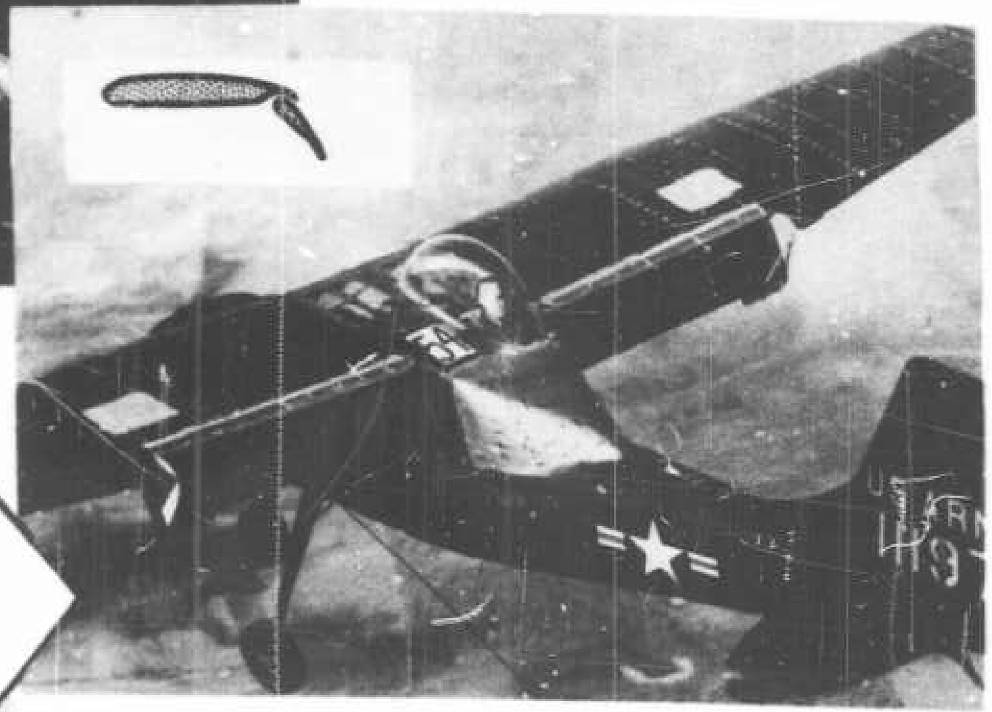

FLOW OVER AIRFOIL WITH MODIFIED SLOTTED FLAP. SAME CONDITION AS ABOVE

FIG. 2

CONFIDENTIAL

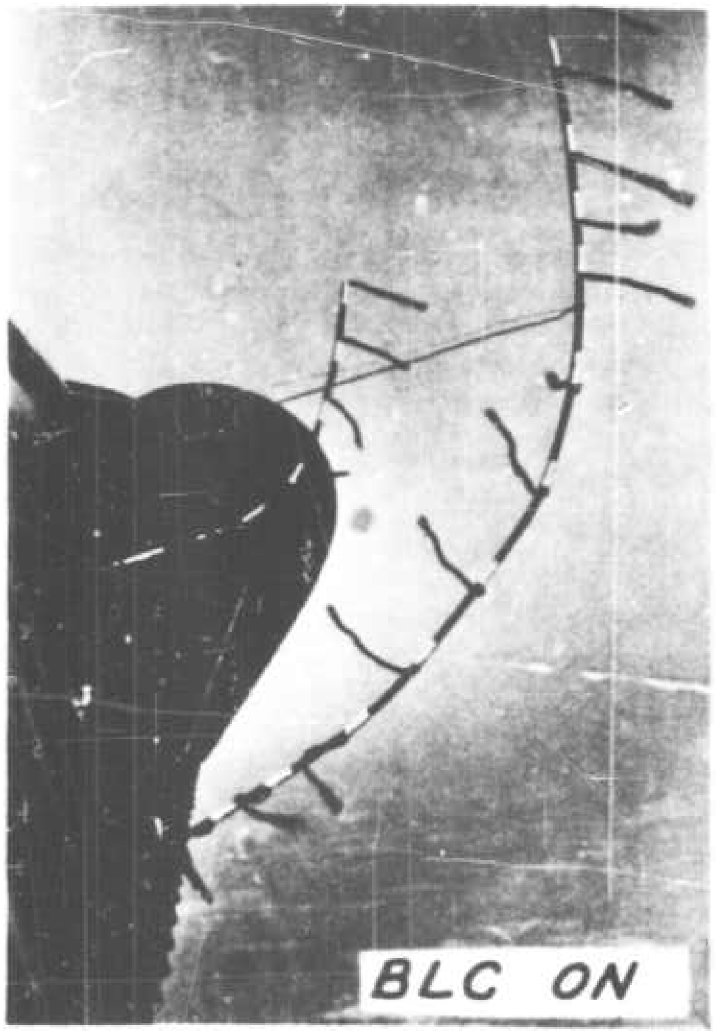

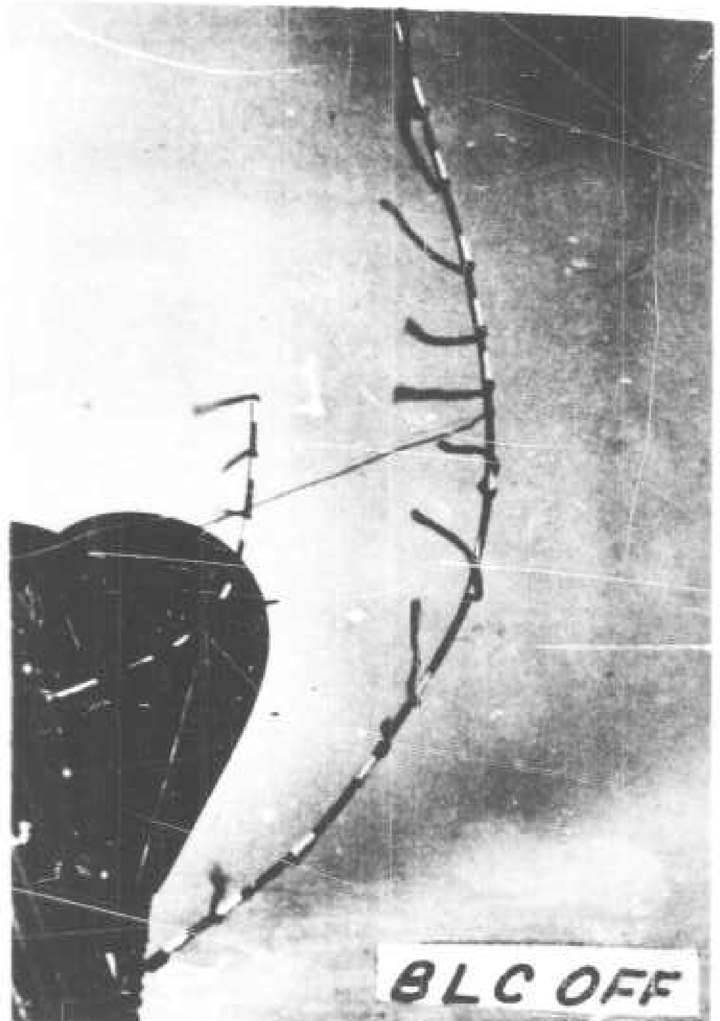

TUFT PHOTOS SHOWING SPATIAL FLOW OVER L-19 AIRFOIL, IDLE POWER, FULL FLAP

FIG. 3

CONFIDENTIAL

BOUNDARY LAYERS ON SLOTTED FLAP

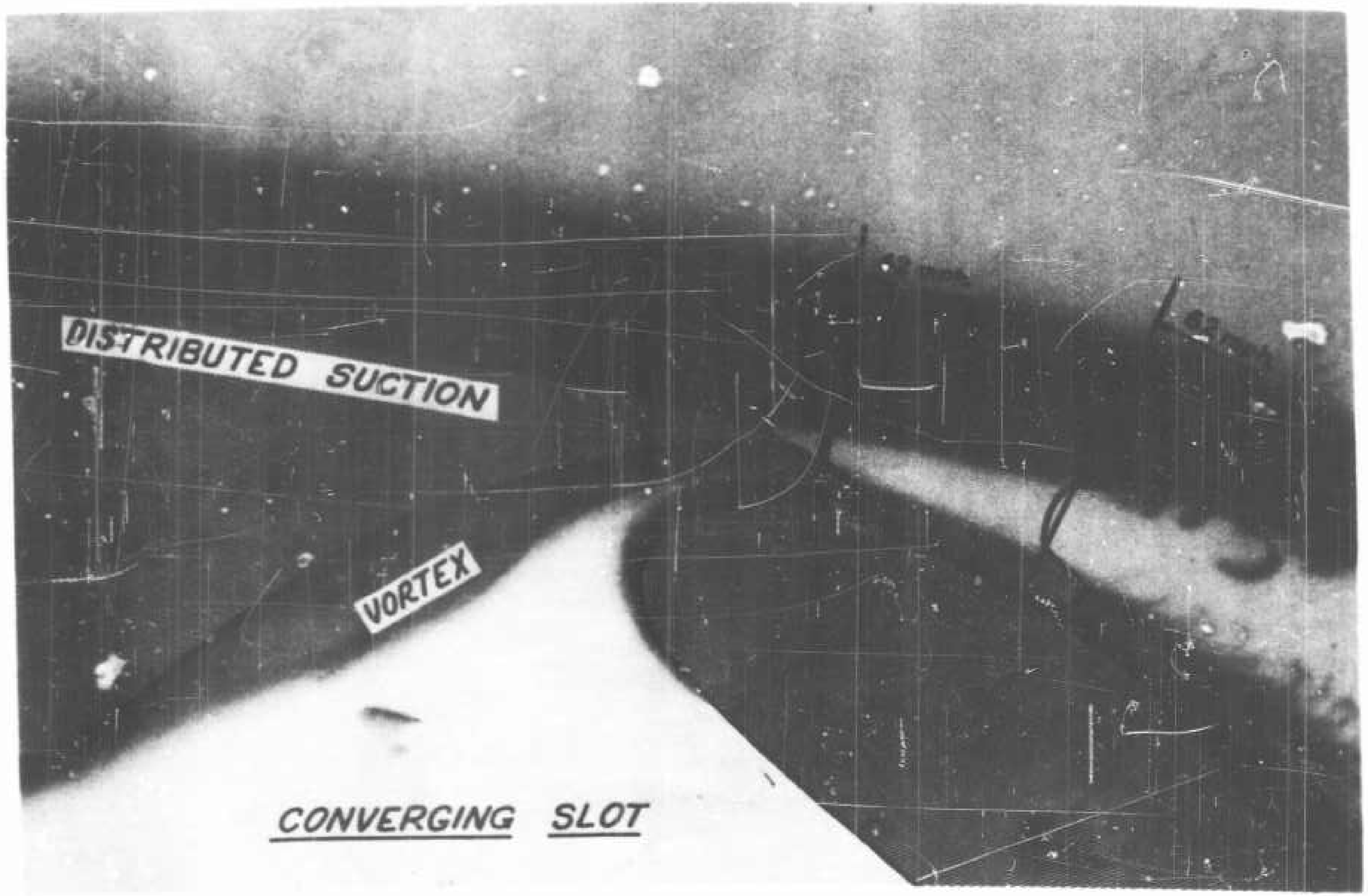

FIG 4

CONFIDENTIAL

BOUNDARY LAYERS ON SLOTTED FLAP

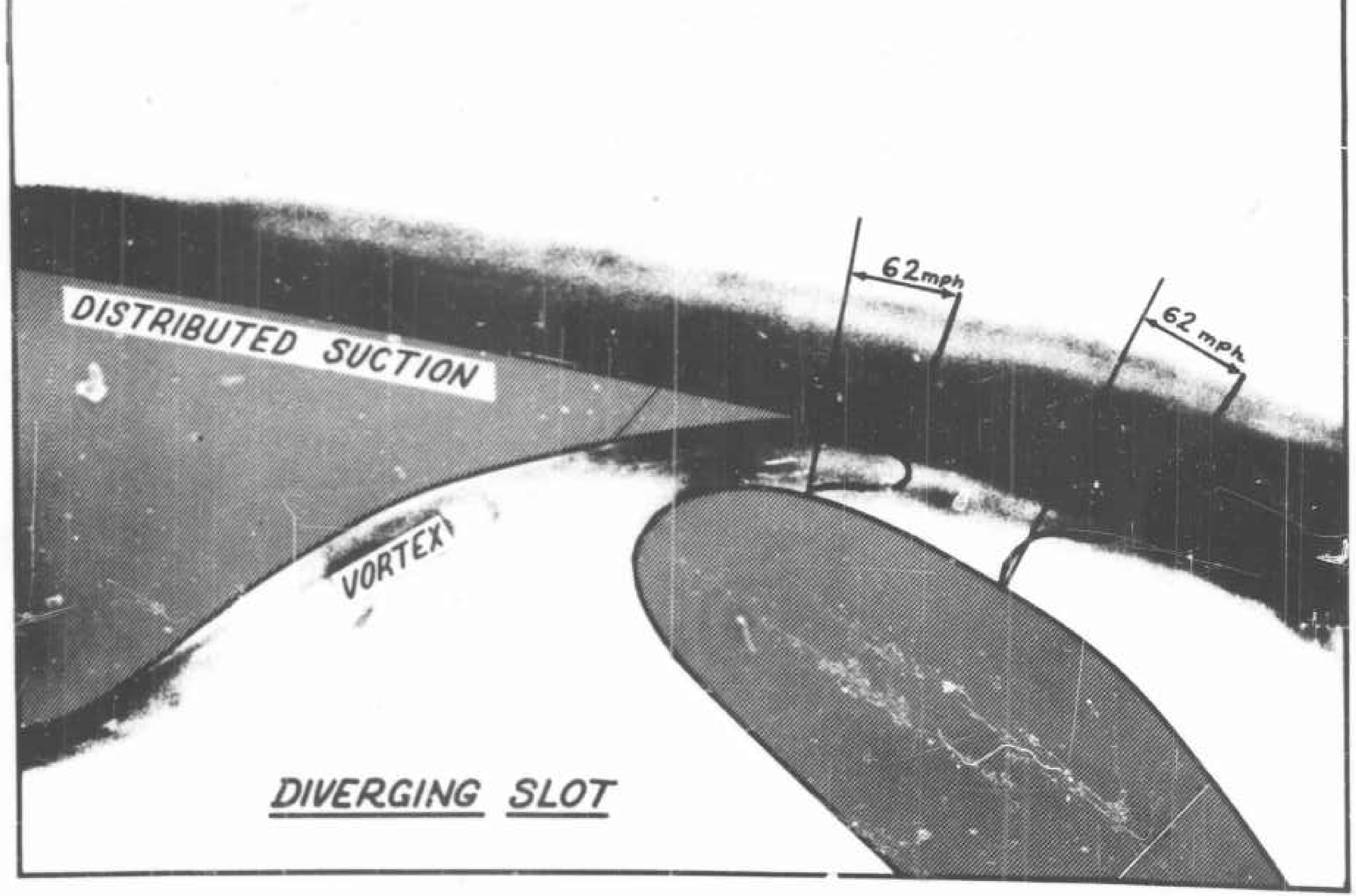

FIG. 5

CONFIDENTIAL

POUNDS OF LIFT DEVELOPED PER HORSEPOWER AS A FUNCTION OF INITIAL POSITION OF DISTRIBUTUTED SUCTION

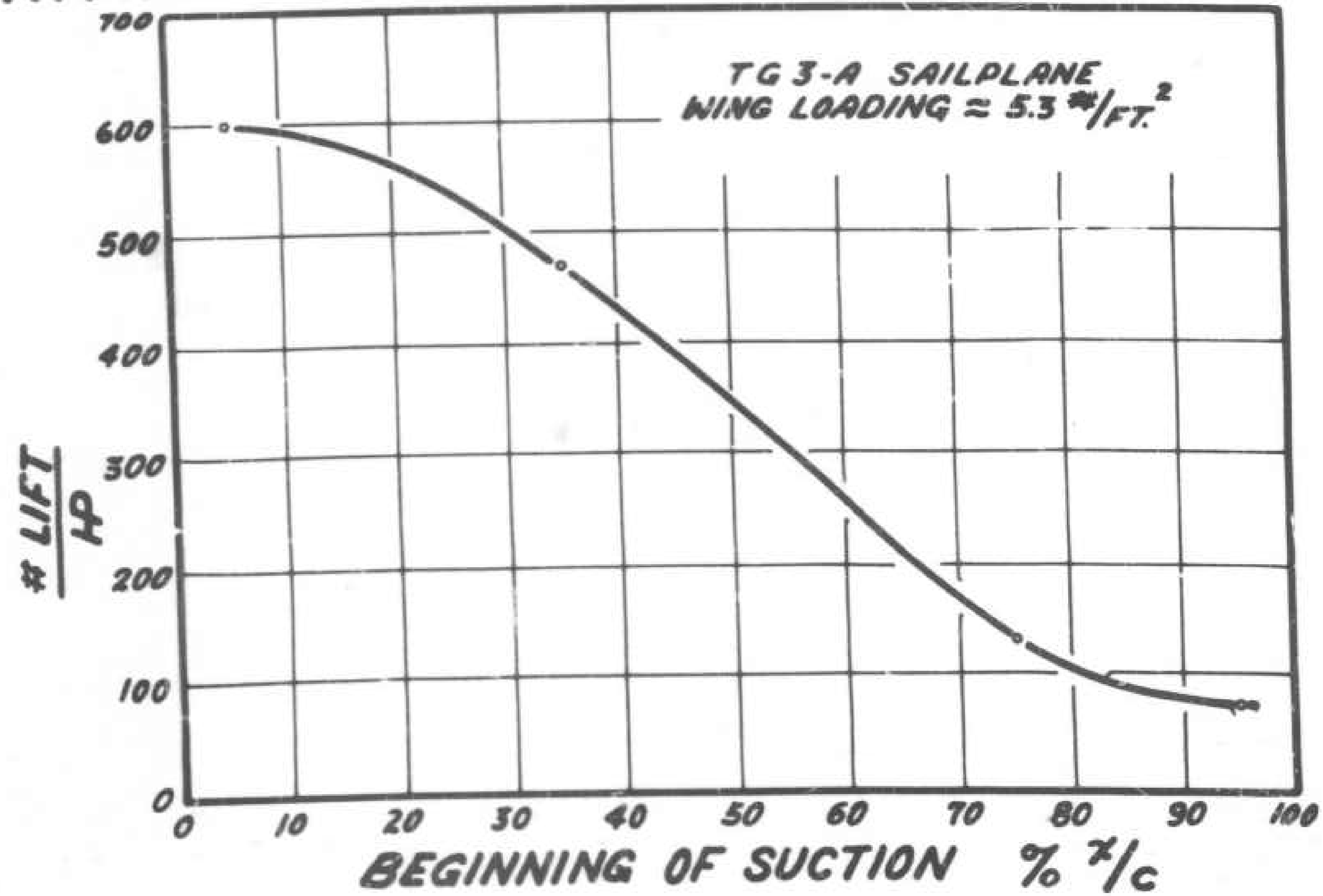

FIG. 6

CONFIDENTIAL

SYSTEM EFFECTIVENESS VERSUS INITIAL POSITION OF CONTROL

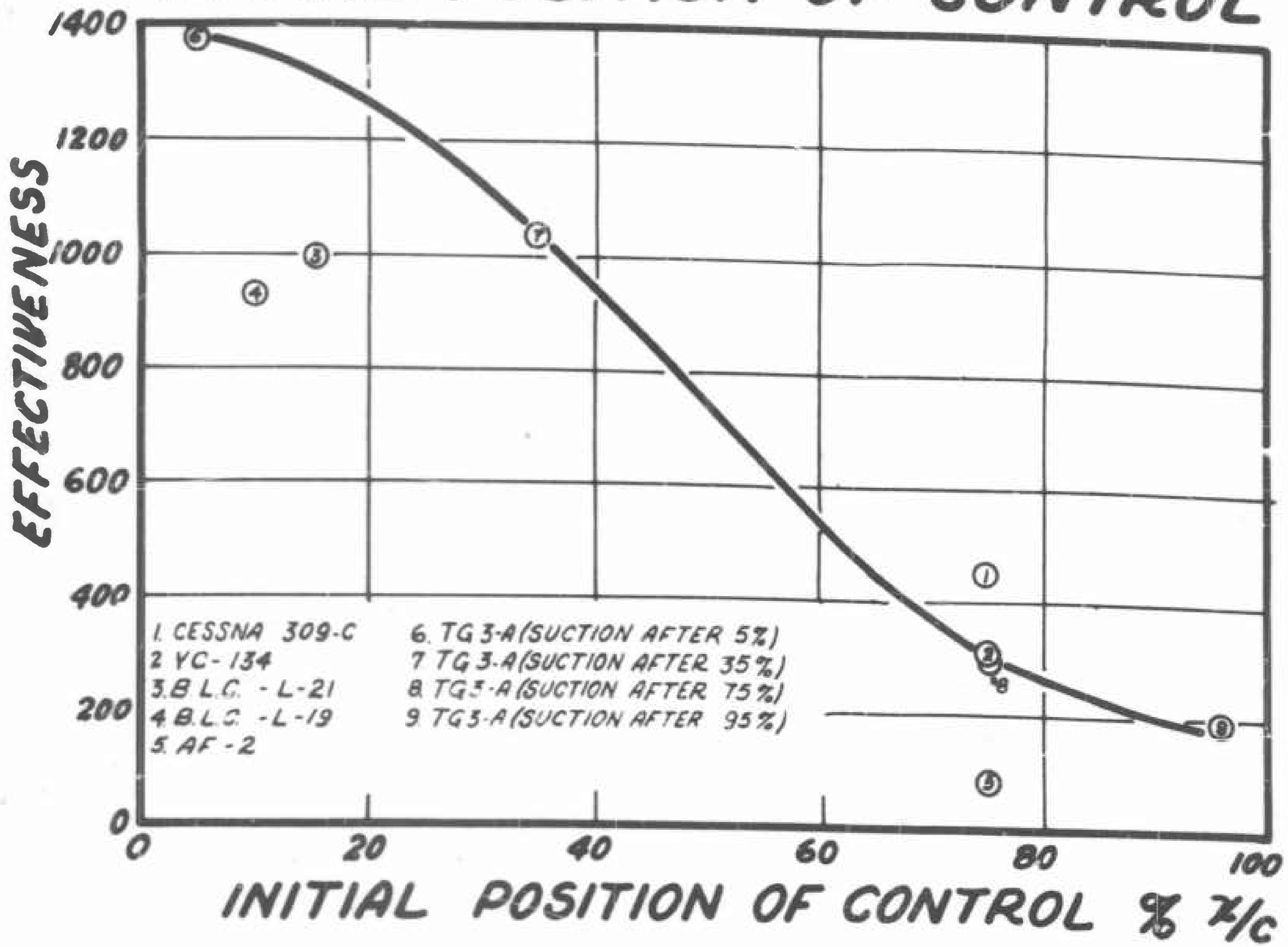

FIG 7

FIG. 8

CONFIDENTIAL

EFFECTIVENESS NOMOGRAPH FOR BOUNDARY LAYER CONTOL SYSTEMS

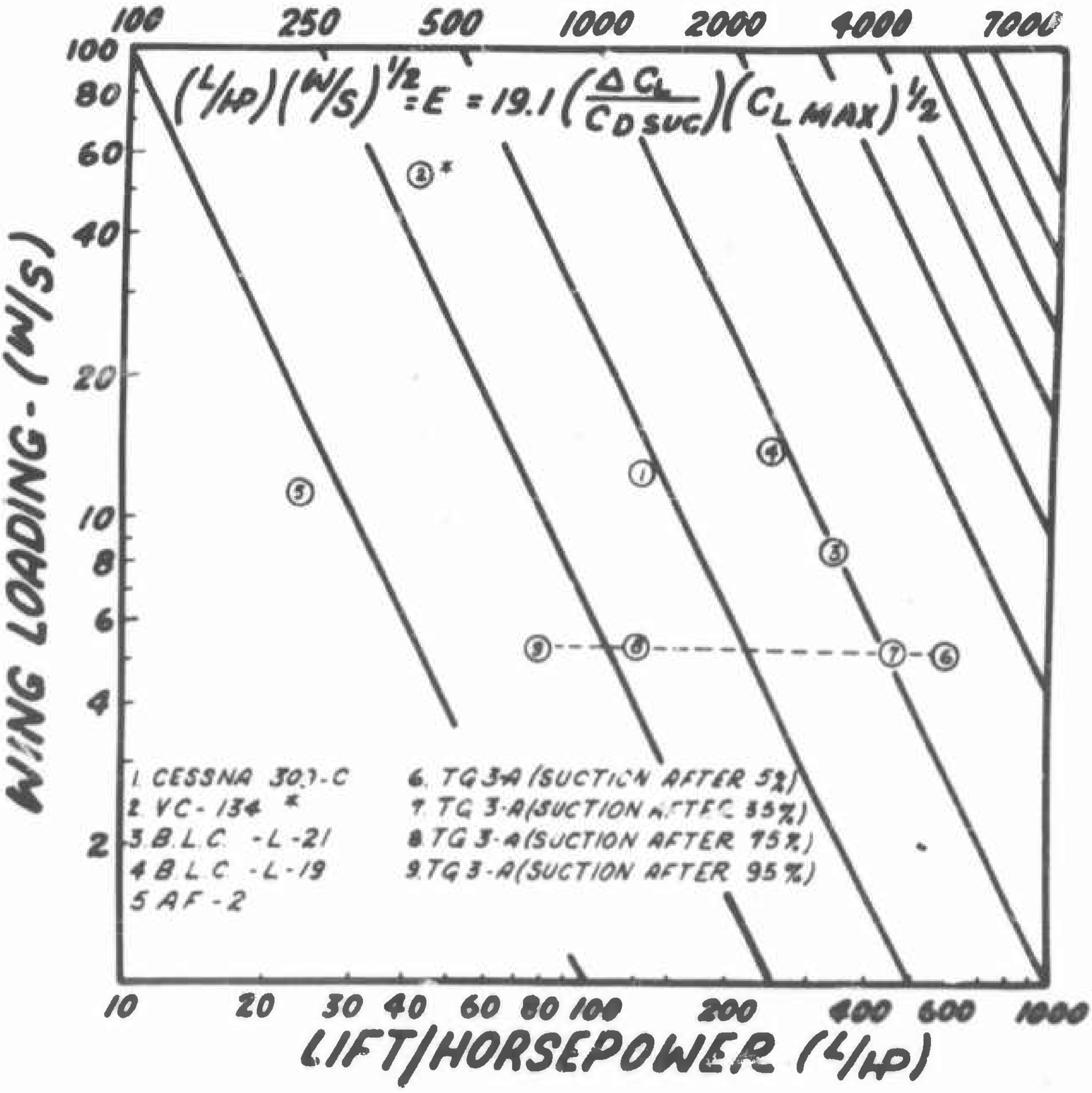

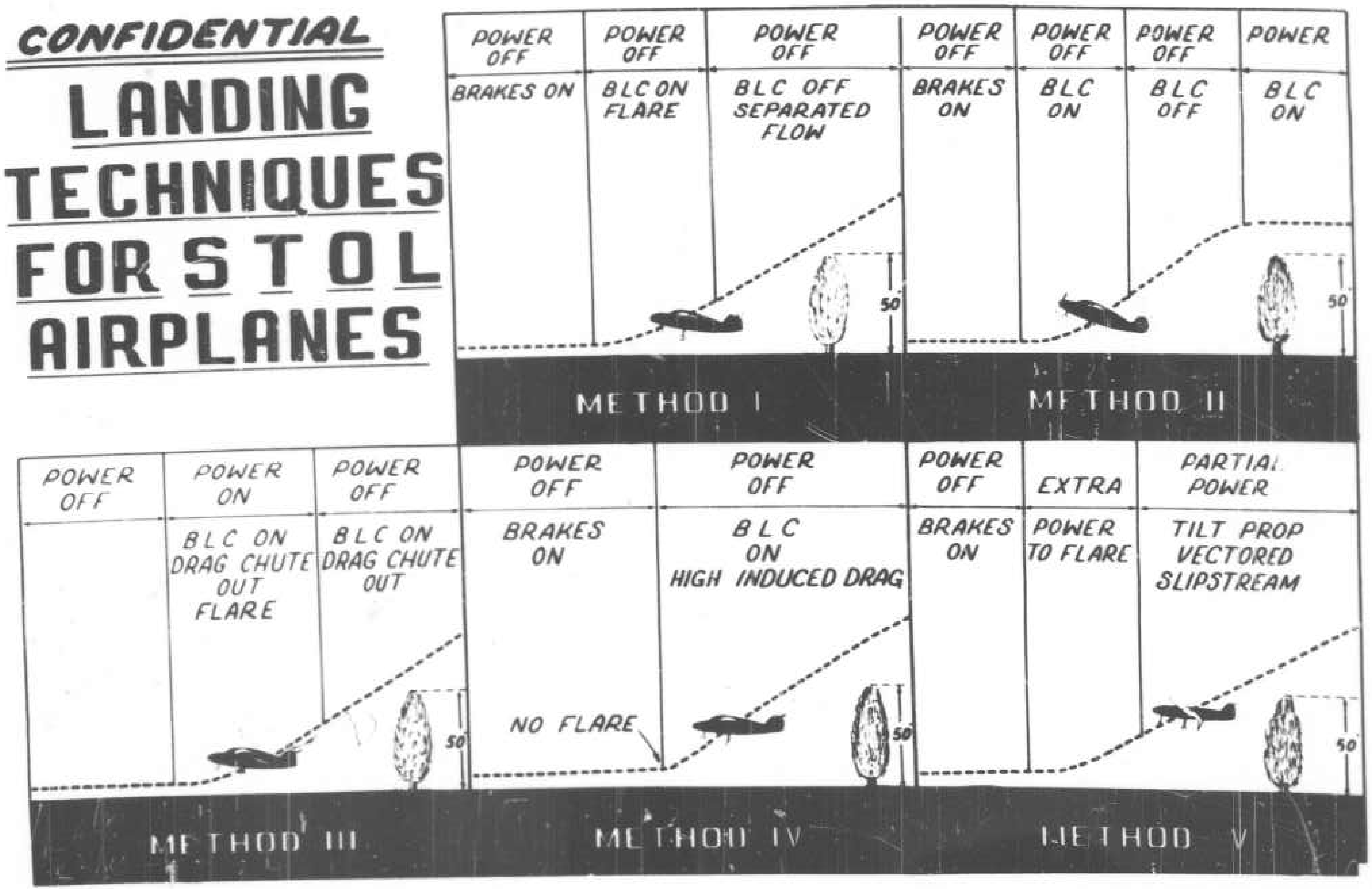
CONFIDENTIAL
LANDING TECHNIQUES FOR STOL AIRPLANES
POWER OFF
BRAKES ON
POWER OFF
BLC ON FLARE
POWER OFF
BLC OFF SEPARATED FLOW
50
METHOD I
POWER OFF
BRAKES ON
POWER OFF
BLC ON
POWER OFF
BLC OFF
POWER
BLC ON
50
METHOD II
POWER OFF
POWER ON
BLC ON DRAG CHUTE OUT FLARE
POWER OFF
BLC ON DRAG CHUTE OUT
50
METHOD III
POWER OFF
BRAKES ON
NO FLARE
POWER OFF
BLC ON HIGH INDUCED DRAG
50
METHOD IV
POWER OFF
BRAKES ON
EXTRA
POWER TO FLARE
PARTIAL POWER
TILT PROP VECTORED SLIPSTREAM
50
METHOD V

FIG. 9

CONFIDENTIAL

L-23A
TOTAL ENERGY VS LANDING DISTANCE

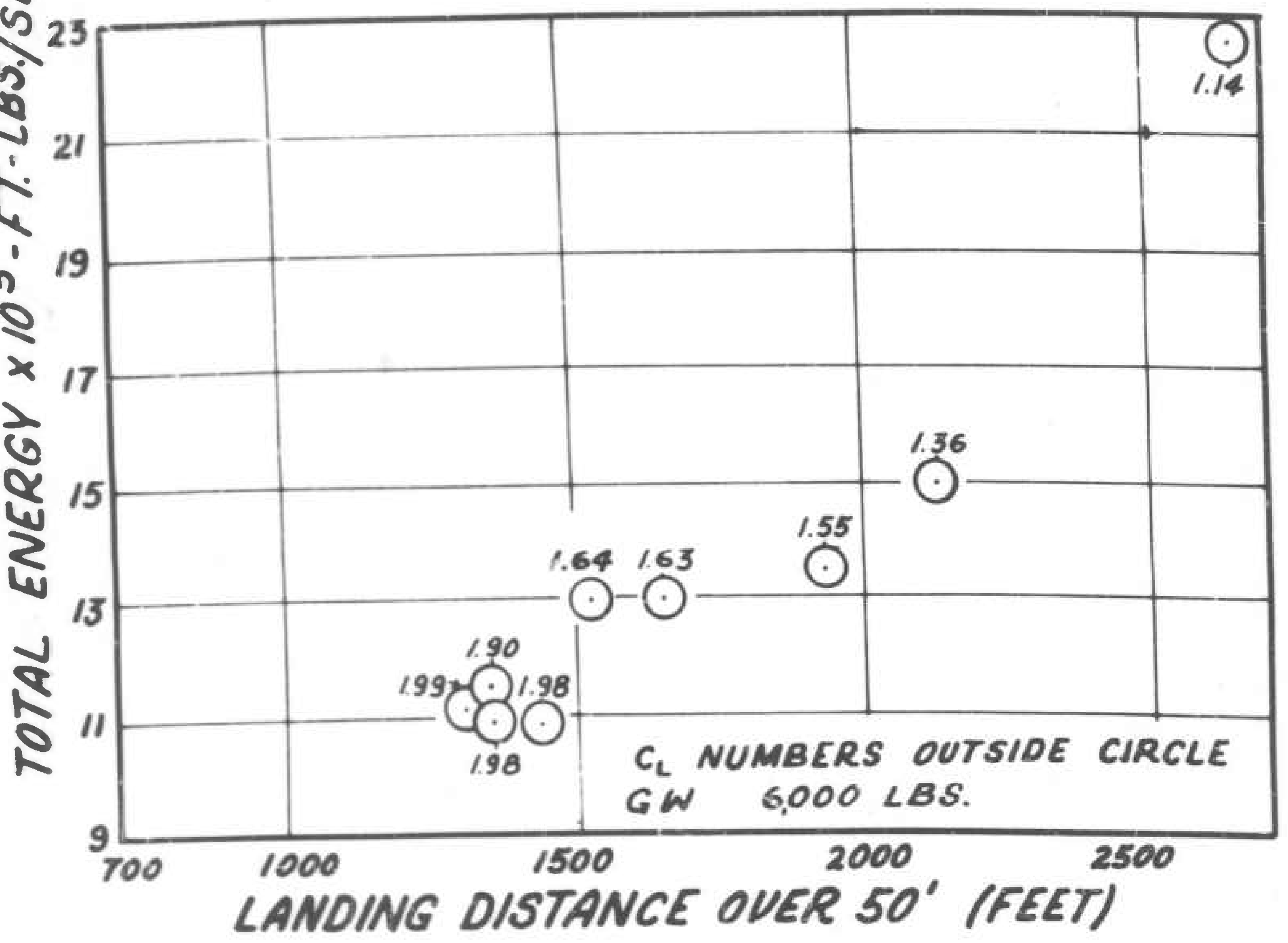

FIG. 10

CONFIDENTIAL

C-123 B
TOTAL ENERGY VS LANDING DISTANCE

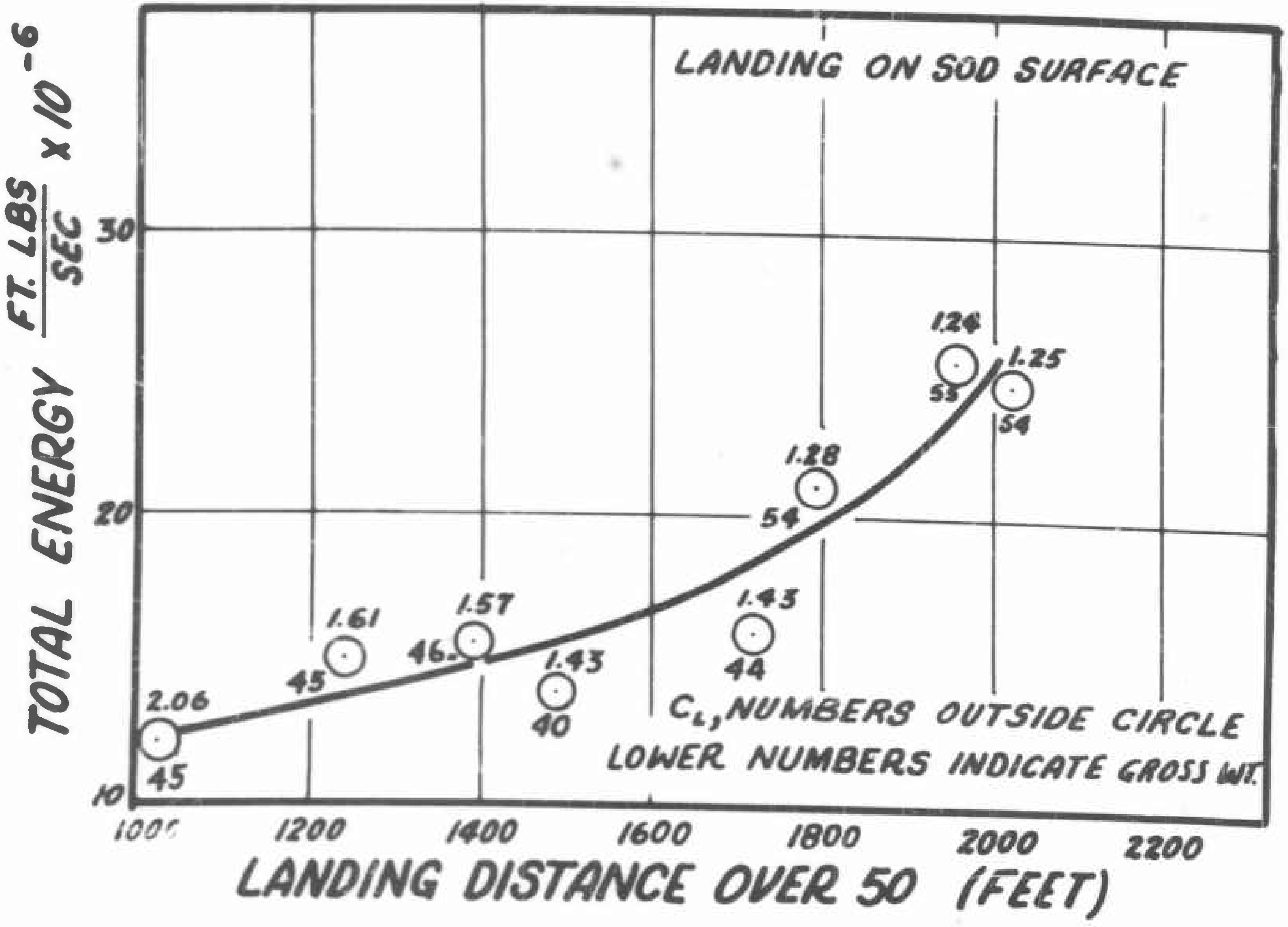

FIG. 11

CONFIDENTIAL

CESSNA MODEL 319 A
C_L VS TOTAL DISTANCE

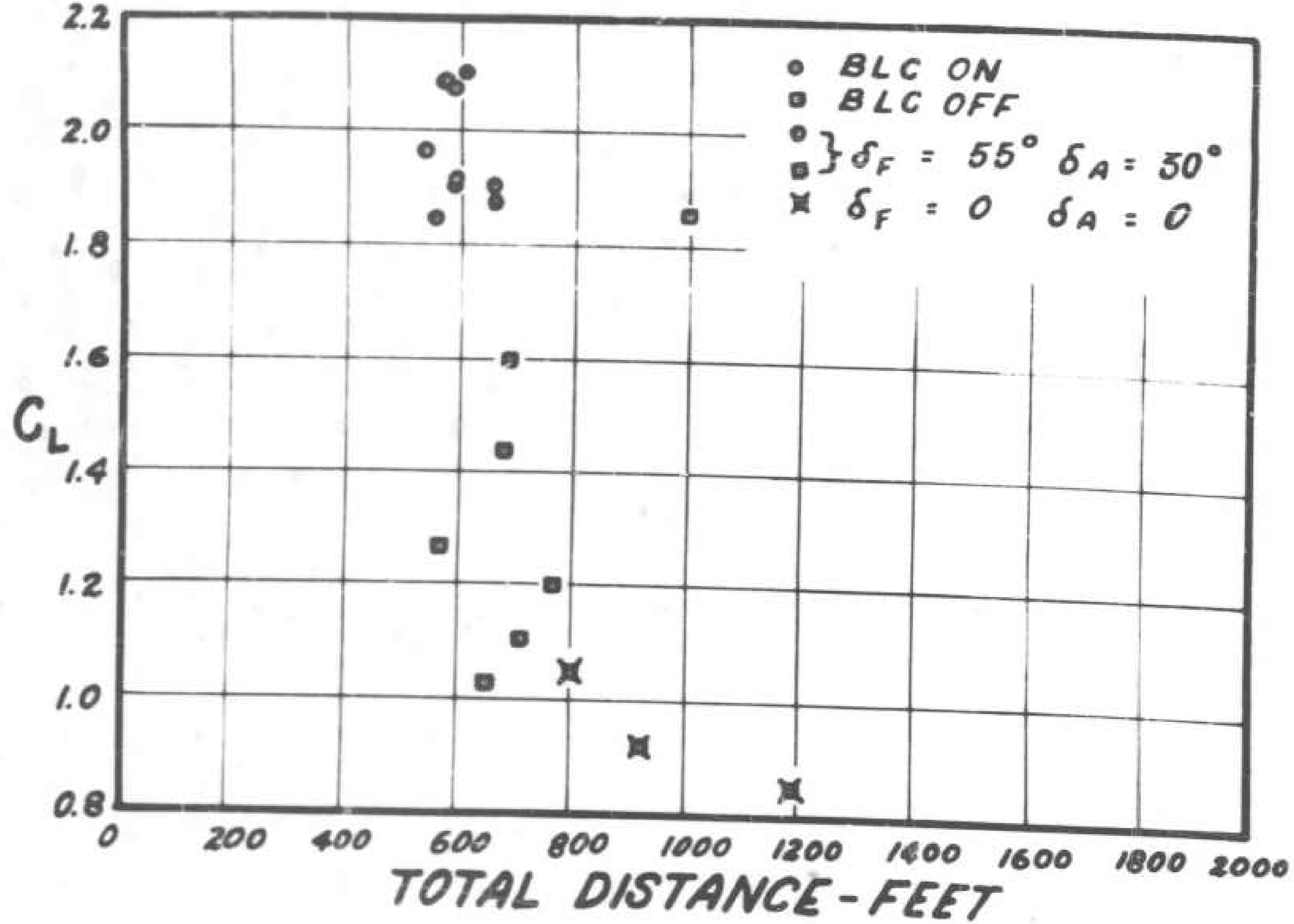

FIG. 12

LIFT RESERVE INDICATOR

CONFIDENTIAL

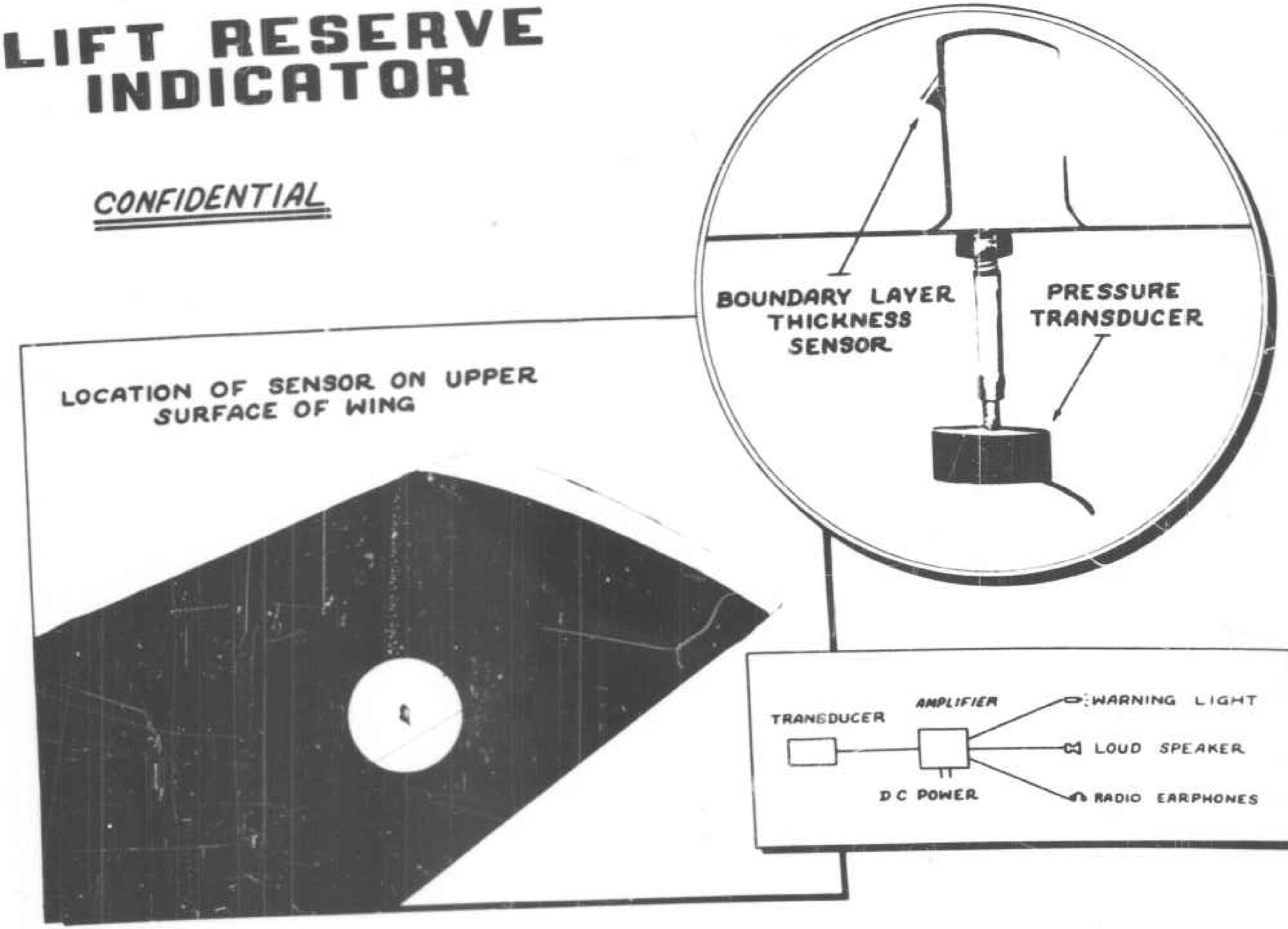

FIG. 13

FIG. 14

CONFIDENTIAL

LIFT RESERVE INDICATOR CALIBRATED ON ARMY L-17B NAVION

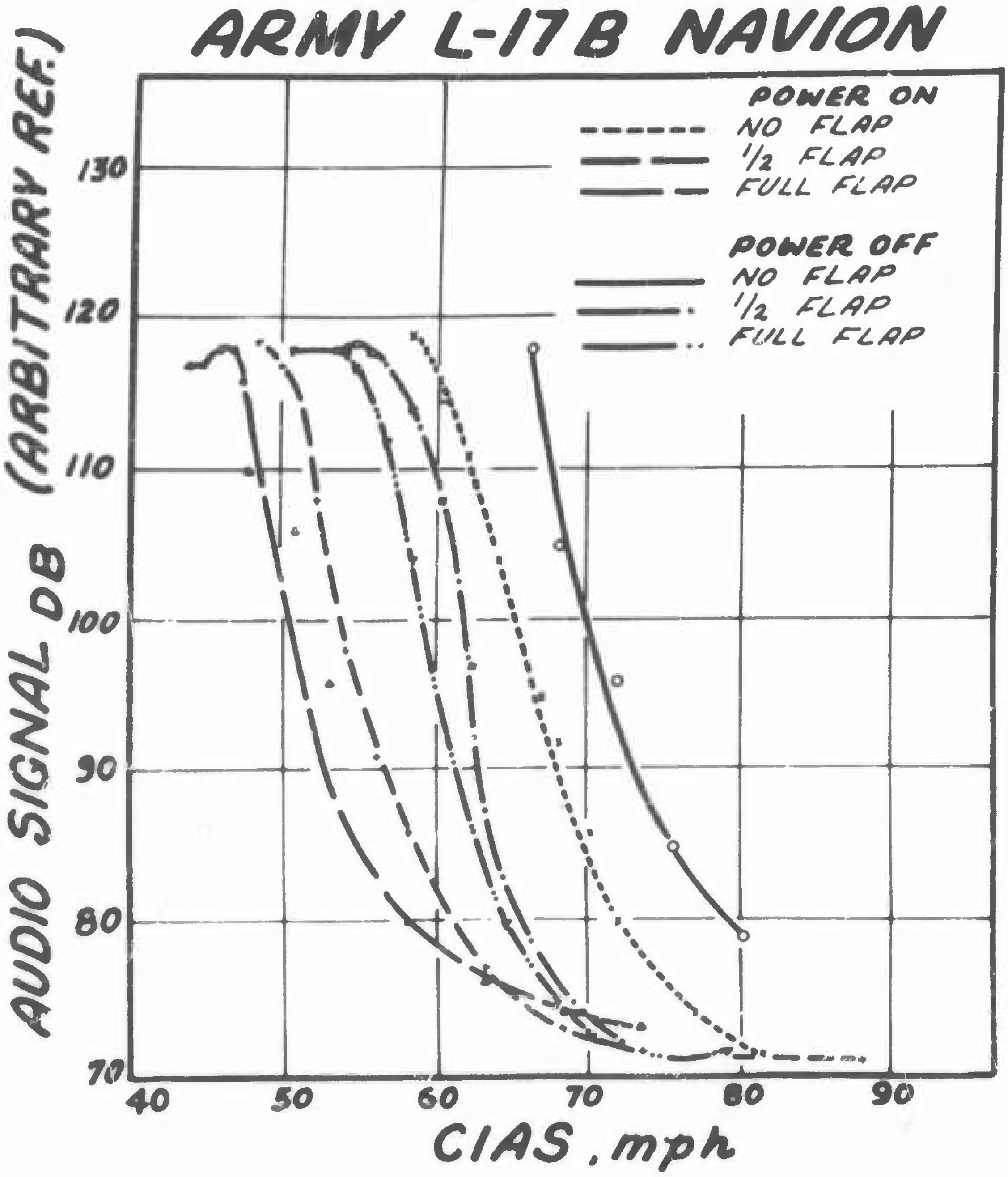

FIG. 15

CONFIDENTIAL

PROPOSED BOUNDARY LAYER CONTROL SYSTEM FOR C-123

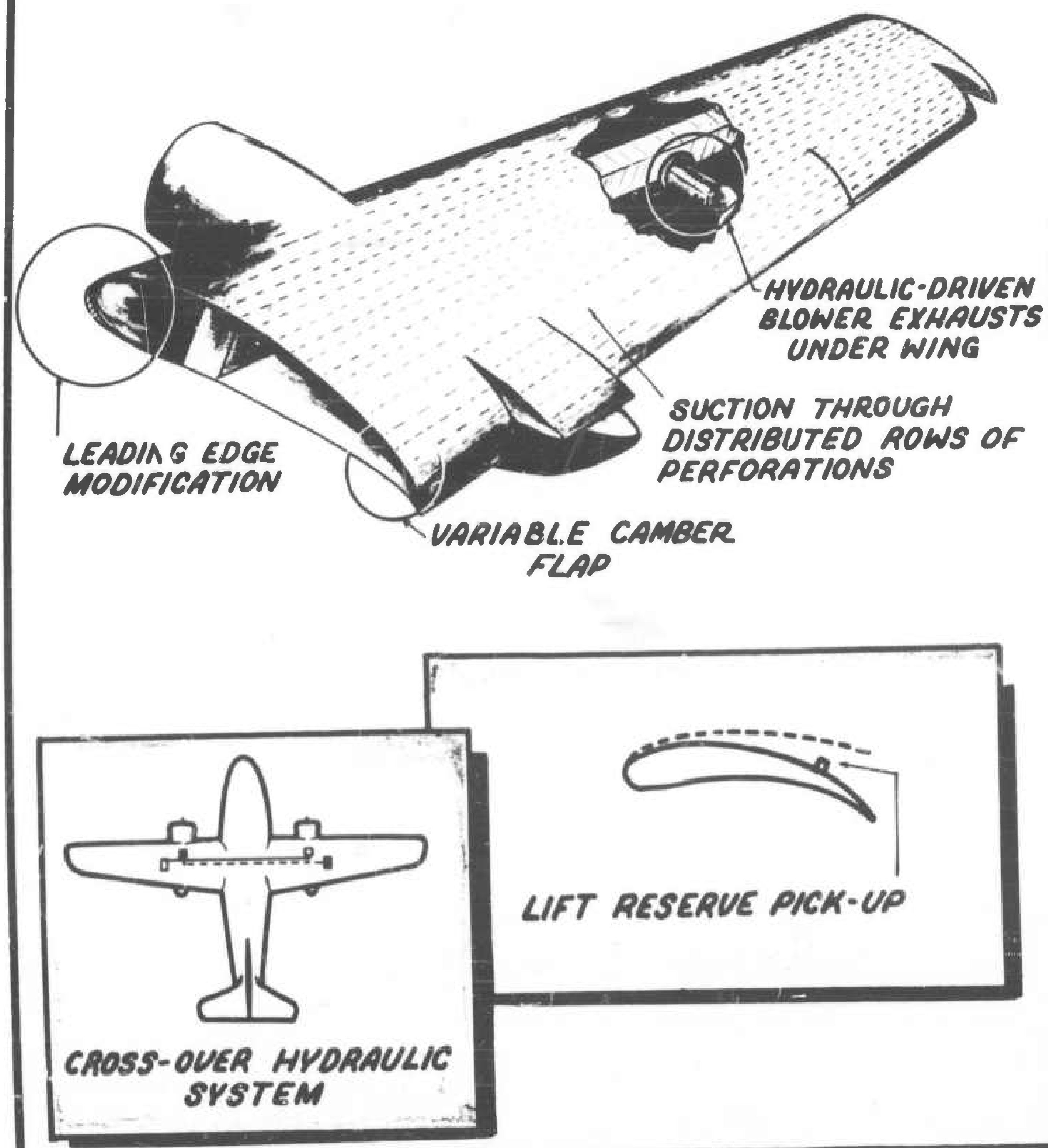

CONFIDENTIAL

EFFECTS AND REQUIREMENTS OF BOUNDARY LAYER CONTROL SYSTEM ON L-23 VERTICAL TAIL SURFACES

	WITHOUT BLC	WITH BLC
PUMP CAPACITY	-	10 CFS FOR EACH PUMP
PUMP PRESSURE	-	7" H_2O FOR EACH PUMP
TOTAL EFFICIENCY	-	60 %
HP REQUIRED	-	1.10 FOR EACH PUMP
C_L RUDDER & FIN	0.66	2.18
SINGLE-ENGINE SPEED	85 MPH	57 MPH
POWER-ON STALL	54 MPH	54 MPH

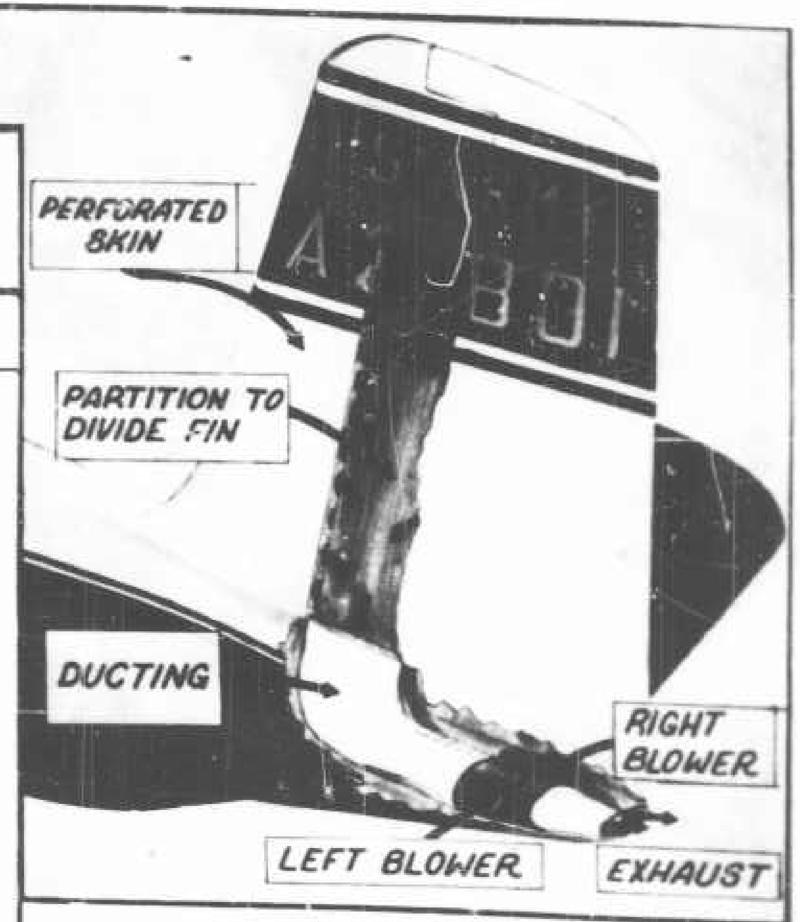

IMPROVEMENT OF SINGLE ENGINE MINIMUM CONTROLLED SPEED

FIG. 16

FIG. 17

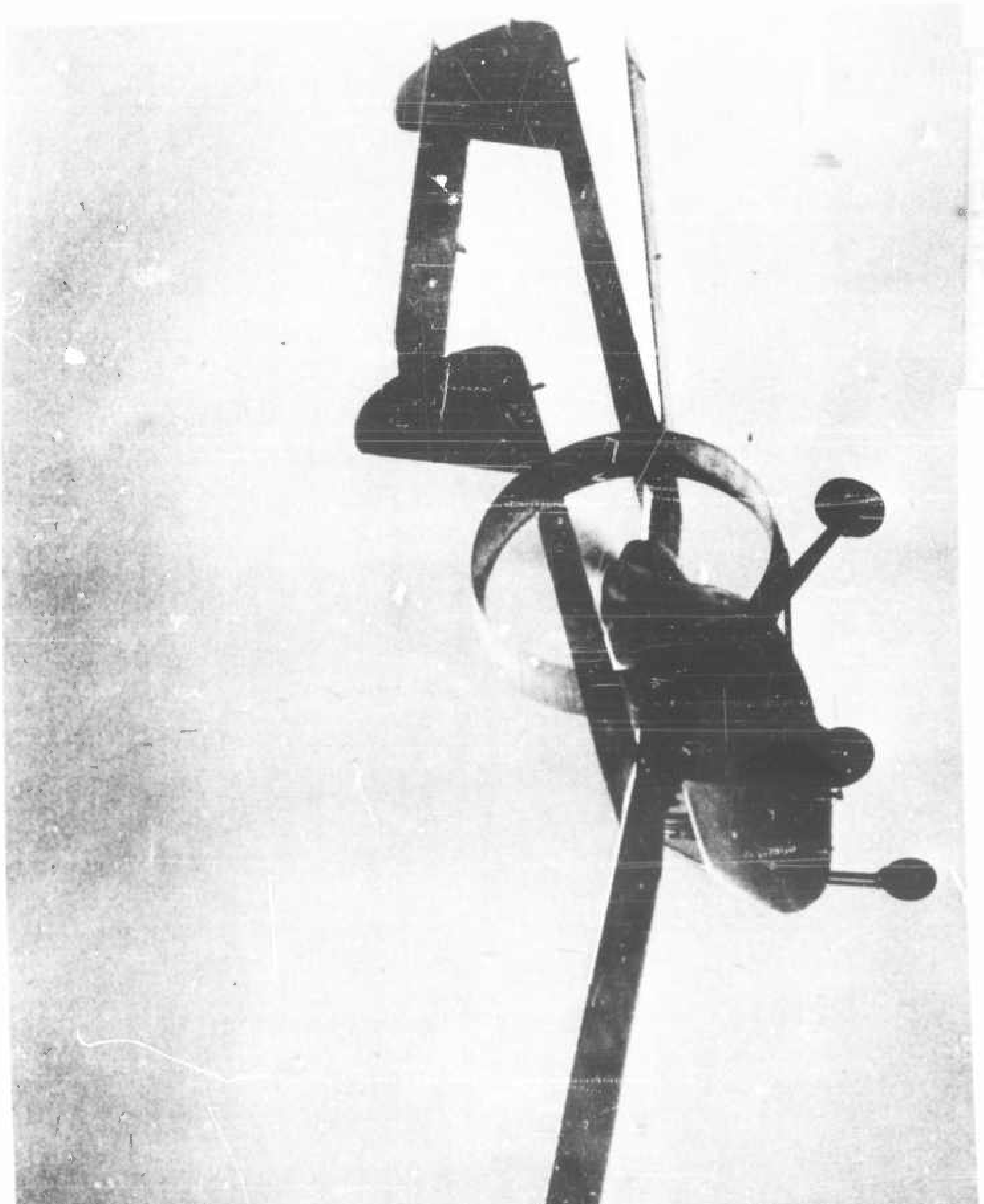

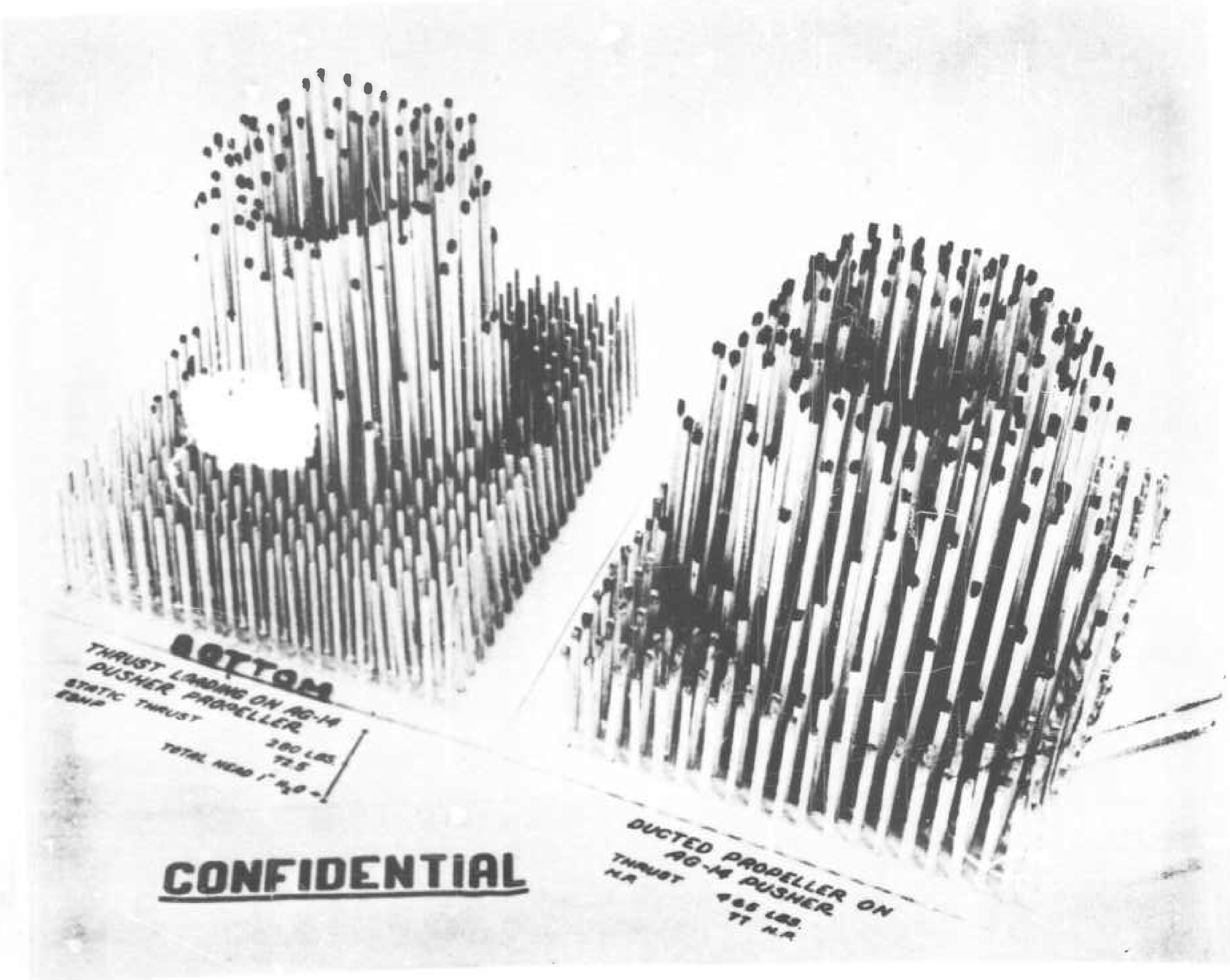
BOTTOM
THRUST LOADING ON AG-14 PUSHER PROPELLER
STATIC THRUST 280 LBS.
RPM 72.5
TOTAL HEAD 1" H2O
DUCTED PROPELLER ON AG-14 PUSHER
THRUST 465 LBS.
H.P. 77 H.P.
CONFIDENTIAL

FIG. 18

CONFIDENTIAL

VARIATION OF STATIC THRUST WITH DISC LOADING FOR SHROUDED AND UNSHROUDED PROPELLERS

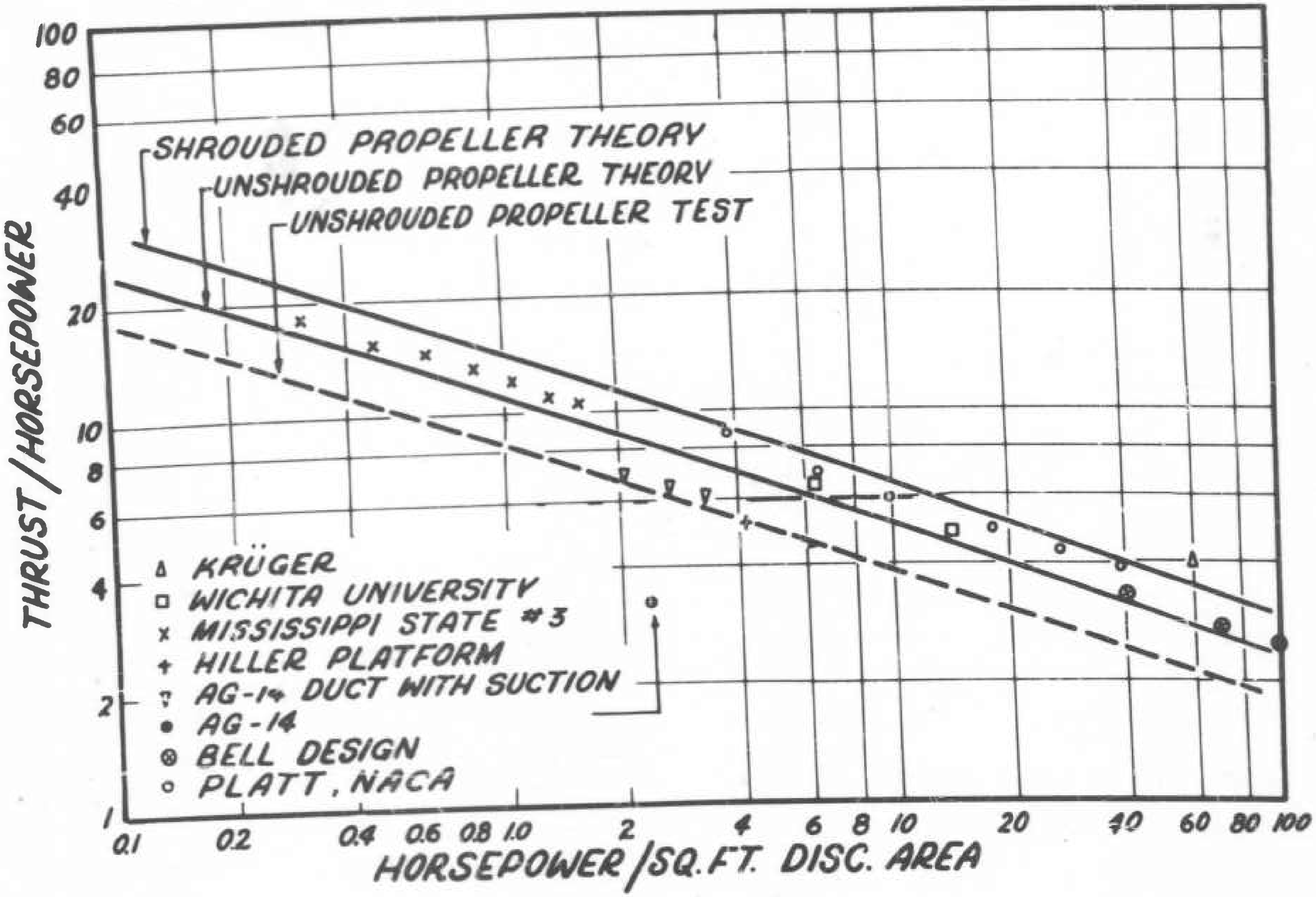

FIG. 19

FIG.2(

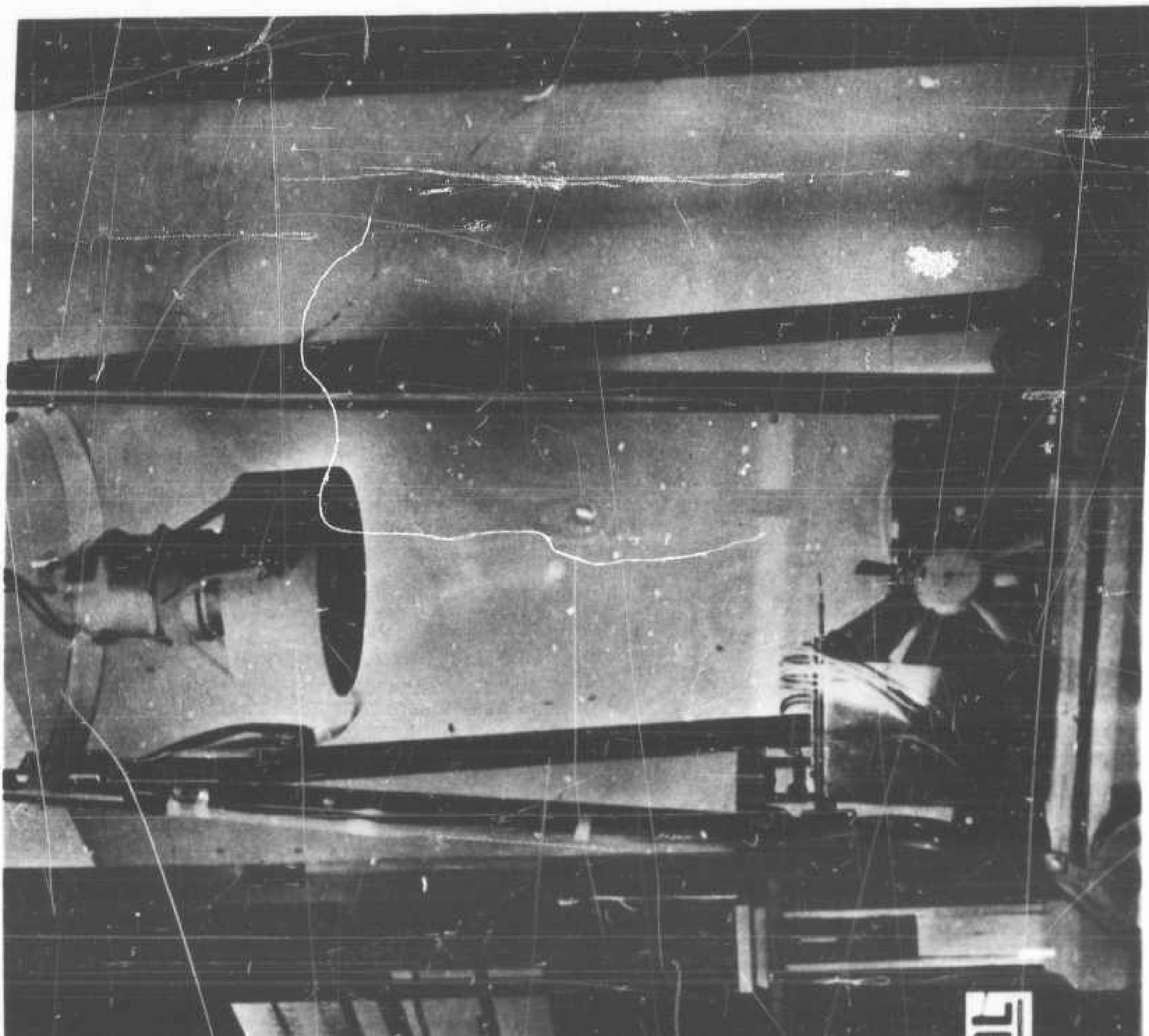

CONFIDENTIAL

SHROUD THRUST VS. TOTAL THRUST

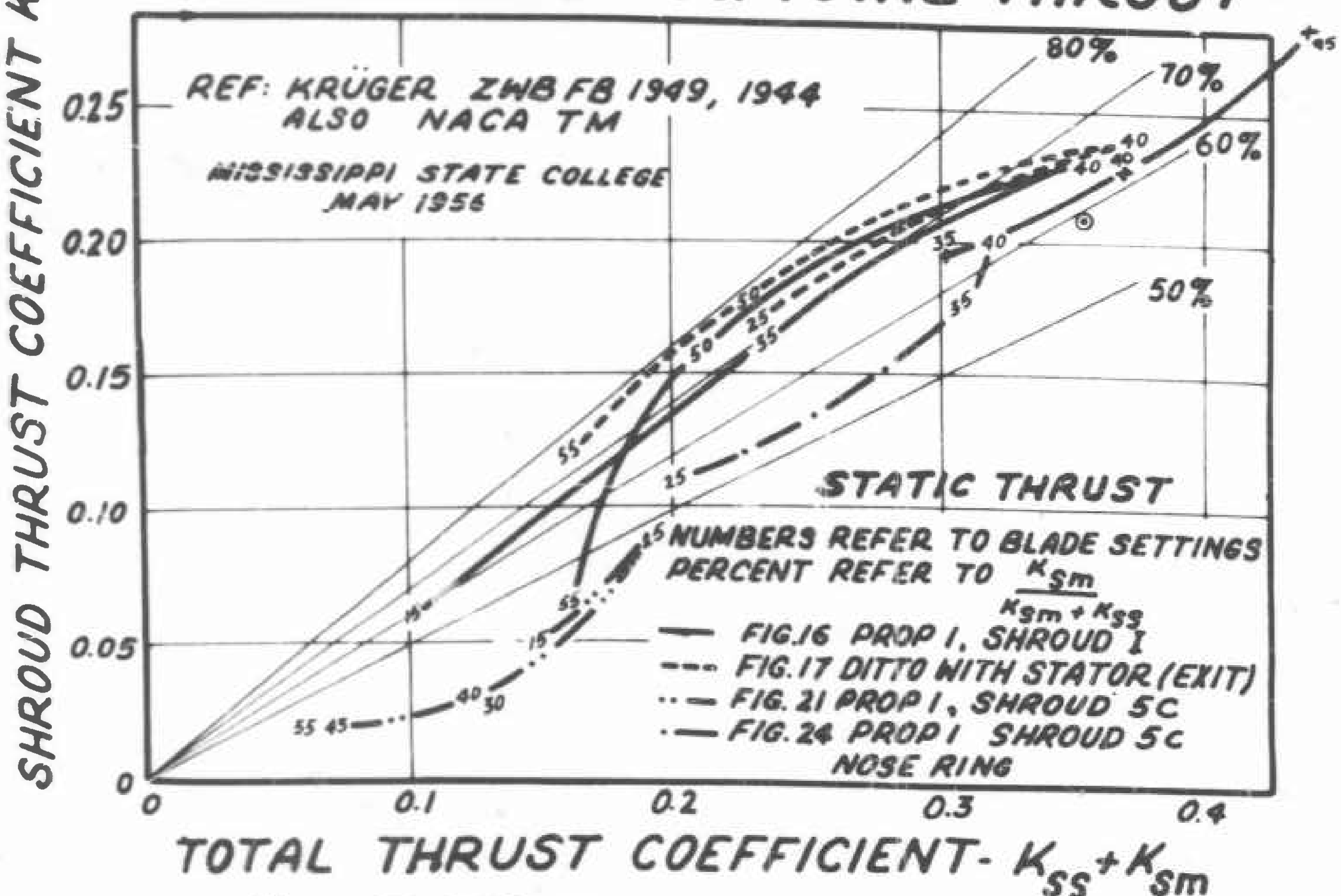

$K_S = \frac{T}{1/2\,\rho u^2 A}$ T = THRUST

u = TIP SPEED OF PROP

A = DISK AREA AT PROP

$K_S = \frac{C_T}{3.87}$

+ PLATT NACA SHORT TAKE-OFF SHROUD

⊙ LONG TAKE-OFF

K_{SS} = THRUST COEFFICIENT OF PROPELLER

K_{Sm} : THRUST COEFFICIENT OF SHROUD

FIG. 21A

CONFIDENTIAL

DUCTED PROPELLER THRUST AG-14 CONSTANT PITCH

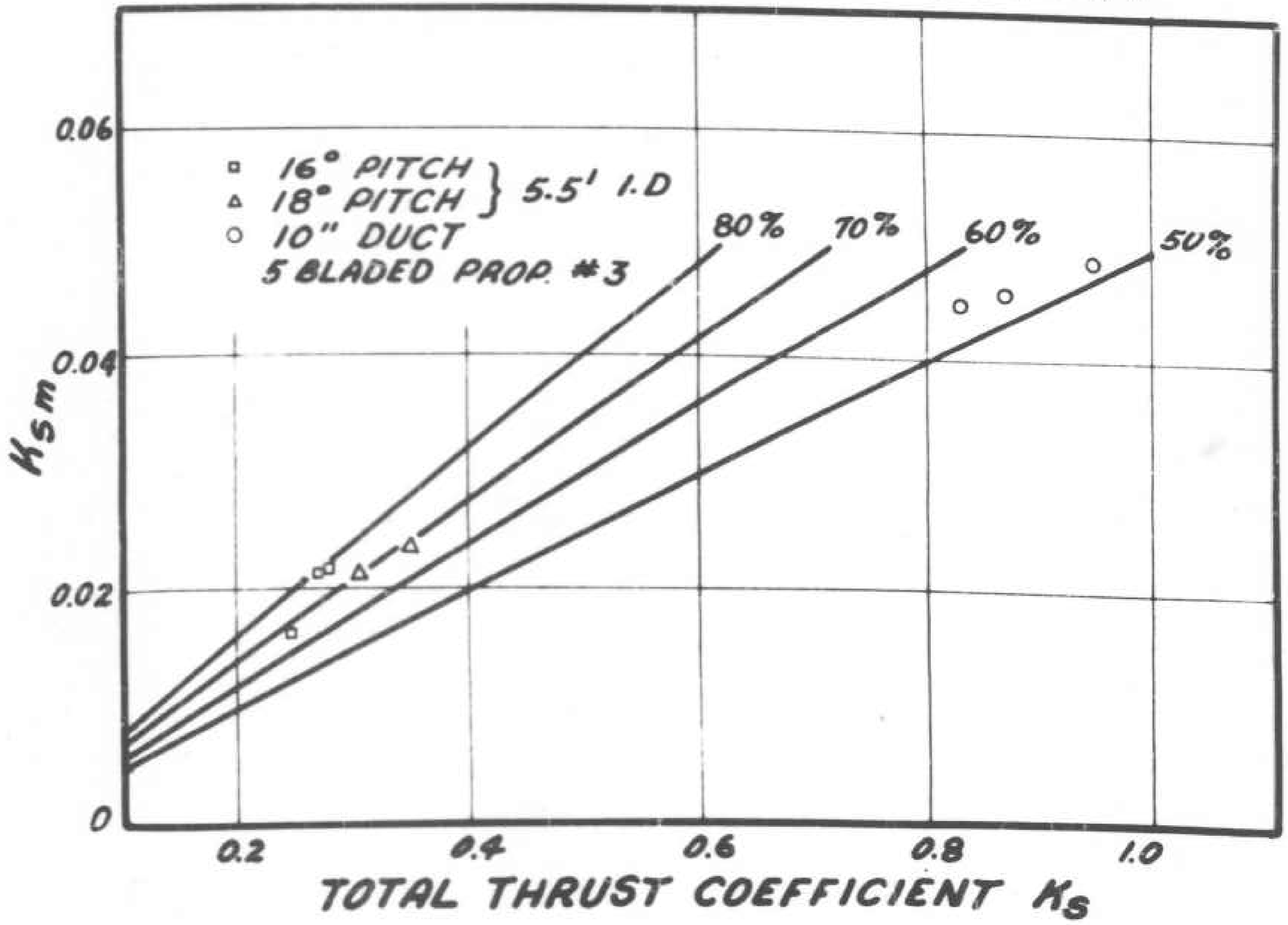

FIG. 21B

FIG.22

CONFIDENTIAL

VELOCITY PROFILE

INLET OF DIFFUSER — OUTLET OF DIFFUSER

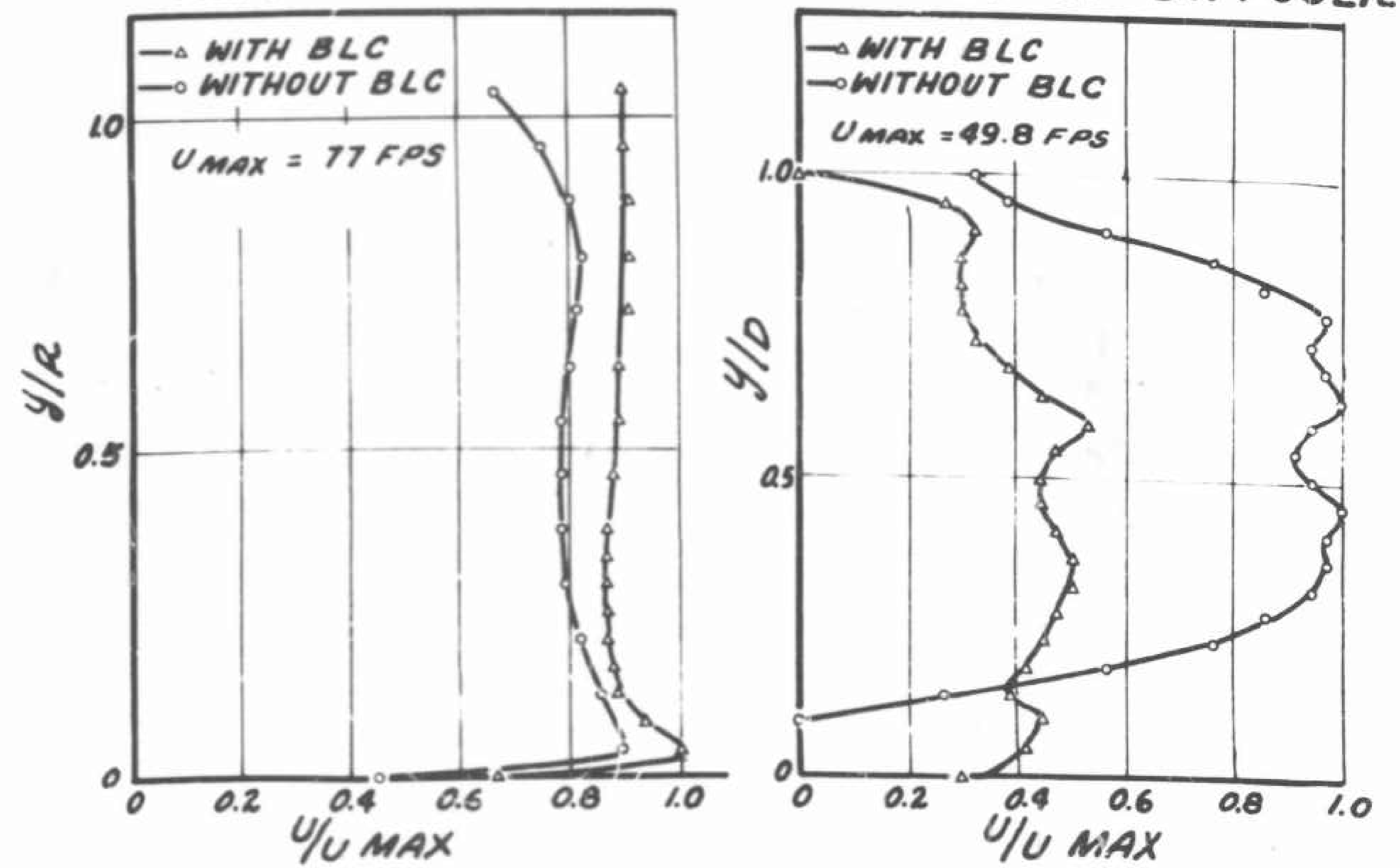

FIG. 23

CONFIDENTIAL

MICROFLASH TUFT PICTURES
SHOWING INFLUENCE OF SUCTION
ON RADIAL FLOW IN BOUNDARY LAYER

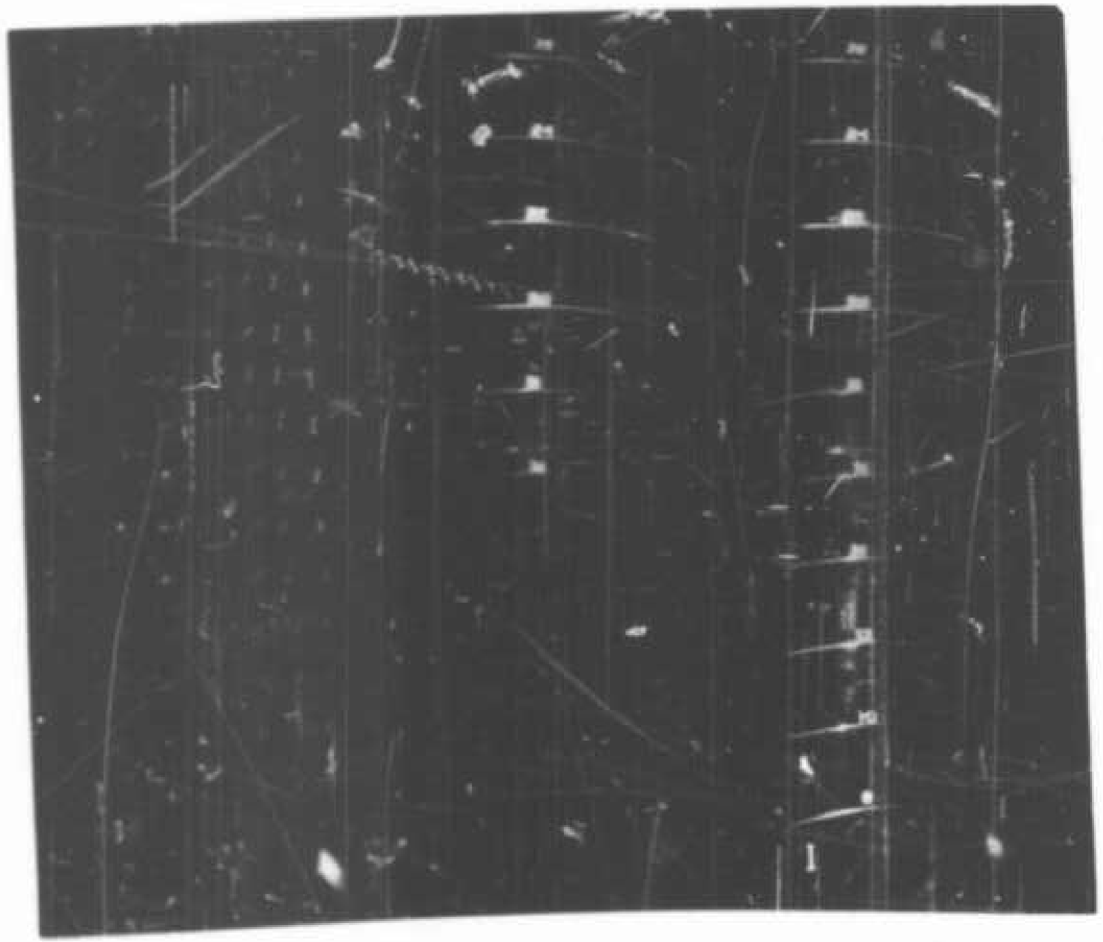

A.	B.	C.
IMPERVIOUS, NO SUCTION	DISTRIBUTED SUCTION $0.58 < \frac{r}{R} < 1.0$	DISTRIBUTED SUCTION FROM HUB TO TIP $0.222 \frac{r}{R} < 1.0$

TUFTS ARE EXTENSIBLE NYLON (HELENCA YARN). THEIR LENGTH YIELDS A MEASURE OF SHEAR.

FIG. 24

CONFIDENTIAL

$C_{n\psi}$ VS C_L

EPB-1 "PLANK" WITH POSITIVELY RAKED TIPS

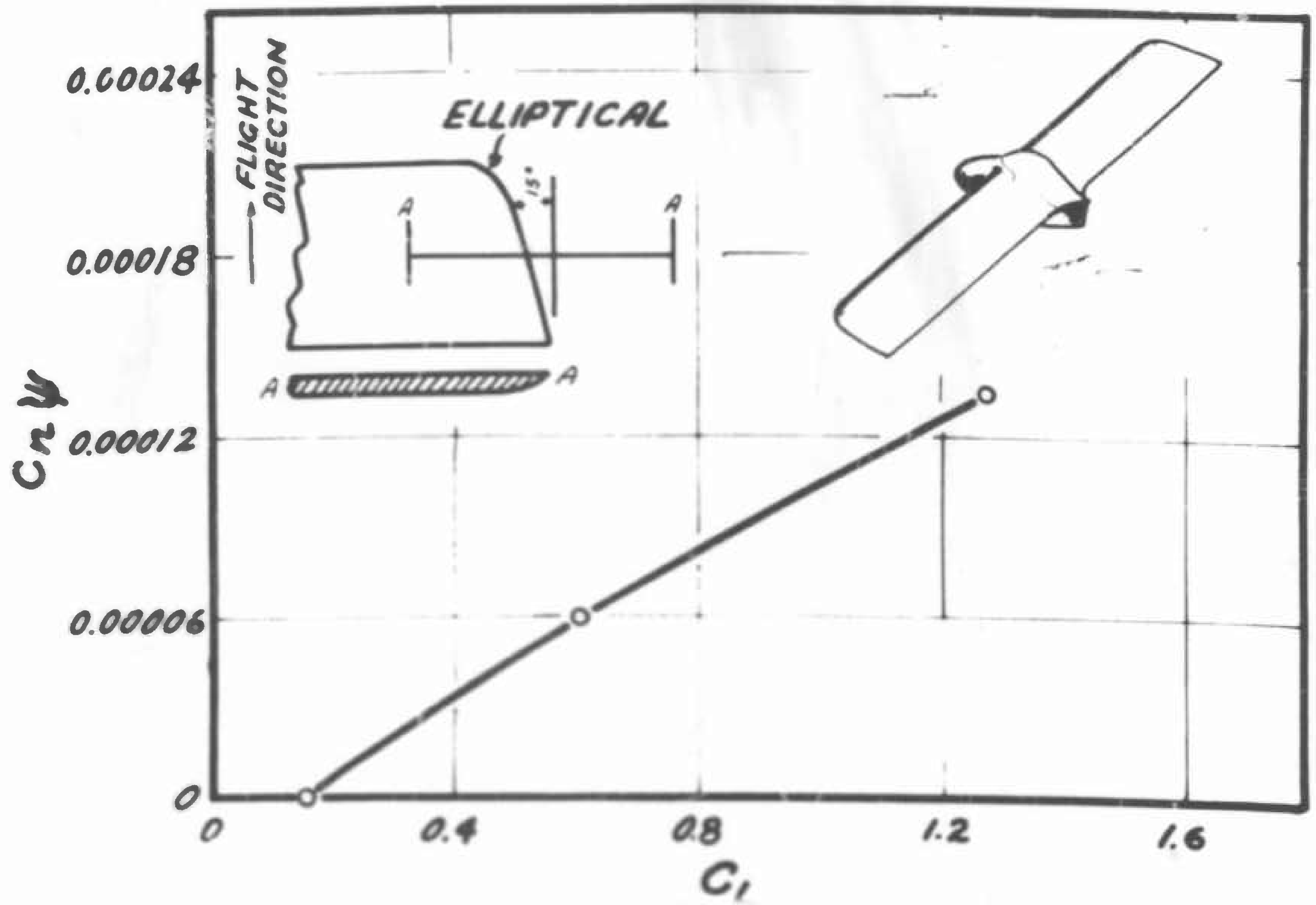

FIG. 2?